Faculty of Engineering

Development of Non-Contact Measurement of Glucose in Urine by Smartphone-Based Laser Refractometry for Continuous Monitoring of Diabetes

Amirul Badiuzzaman

Master of Engineering
2025

Development of Non-Contact Measurement of Glucose in Urine by Smartphone-Based Laser Refractometry for Continuous Monitoring of Diabetes

Amirul Badiuzzaman

A thesis submitted

In fulfillment of the requirements for the degree of Master of Engineering

(Non-Intrusive Measurement Techniques)

Faculty of Engineering
UNIVERSITI MALAYSIA SARAWAK
2025

DECLARATION

I declare that the work in this thesis was carried out in accordance with the regulations of Universiti Malaysia Sarawak. Except where due acknowledgements have been made, the work is that of the author alone. The thesis has not been accepted for any degree and is not concurrently submitted in candidature of any other degree.

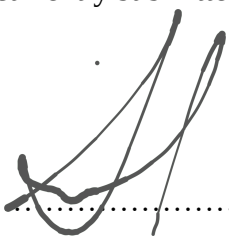

……

Signature

Name: Amirul Badiuzzaman

Matric No.: 22020262

Faculty of Engineering

Universiti Malaysia Sarawak

Date : 15th May 2025

ACKNOWLEDGEMENT

First and foremost, syukur alhamdulillah for this opportunity to pursue my dream of furthering my studies in the mechanical engineering field. I cannot express enough of my deepest gratitude to my supervisors, Assoc. Prof. Ir. Dr. Khairul Fikri bin Tamrin and Assoc. Prof. Dr. Muhammad Hamdi bin Mahmood for their invaluable guidance, support, and encouragement throughout the course of this research. Without a doubt, their expertise and insightful feedback have been instrumental in shaping this thesis.

I am also grateful to the faculty members of Fakulti Kejuruteraan Universiti Malaysia Sarawak for providing me with the necessary resources and opportunities to pursue my studies. A special thanks to Advanced Pathology Lab Sdn. Bhd. and Penjara Puncak Borneo for their technical support and assistance during the experimental phase of my research.

My heartfelt appreciation goes to my family and friends, whose support, patience, and motivation have sustained me throughout this journey. Their belief in me has been a constant source of inspiration.

I would like to extend my deepest gratitude to my girlfriend, Dr Zhalika Dianah for her unwavering love, patience, and support throughout this journey. Her encouragement and understanding during challenging times have been invaluable, and I am deeply grateful for her presence in my life.

Lastly, I would like to acknowledge Sarawak Digital Economy Corporation Berhad (SDEC) for their financial support, without which this research would not have been possible.

To all who contributed to this work, directly or indirectly, I extend my deepest thanks.

ABSTRACT

Diabetes mellitus is a global health issue affecting millions of people, requiring regular glucose level monitoring. Current non-invasive methods include urinalysis (colorimetry and biosensors) which are laboratory-based and lack user-friendliness, limiting their practicality for continuous glucose monitoring. Although promising, research on smartphone-integrated laser refractometry for glucose detection remains limited. To address this need, a non-contact smartphone-based laser refractometer for glucose monitoring was developed. This prototype measures the refractive indices of urine by analyzing the refracted length of a laser line, which is correlated with fasting blood glucose concentrations. The proposed prototype uses a smartphone to capture a relatively high resolution images of a laser line caused by total internal reflection through the rod and refraction caused by the urine. Assessments were made through a series of controlled glucose concentrations, varying turbidities, different volumetric samples, and a shelf-life. Volumetric and shelf-life assessments showed no effect to the results whereas as turbidity assessments proved the proposed prototype is limited to 57 nephelometric turbidity units (NTU) of the urine samples. Results of fasting glucose levels measured in urines using the developed system were compared to fasting blood glucose laboratory results, yielding with correlation coefficients of 0.89 and a sensitivity of 4.8 mg/dL. The system is inexpensive, making it accessible, and is suitable for telemedicine applications, providing remote monitoring options for patients. This approach paves the way for clinically crucial glucose detection in diabetics without the need for invasive finger-prick blood sampling.

Keywords: Laser optical measurement, refractometer, non-invasive, glucose monitoring, smartphone

Pembangunan Pengukuran Tanpa Sentuhan Glukosa dalam Urin oleh Refraktometri Laser Berasaskan Telepon Pintar untuk Pemantauan Berterusan Diabetes

ABSTRAK

Diabetes mellitus merupakan isu kesihatan global yang menjejaskan jutaan orang yang memerlukan pemantauan tahap glukosa secara berkala. Kaedah tidak invasif termasuklah analisis air kencing (colorimetry dan biosensor) yang memerlukan peralatan makmal dan kurang mesra pengguna. Ini membataskan pemantauan glukosa secara berterusan dan tidak praktikal. Penyelidikan mengenai refraktometri laser secara bersepadu menggunakan telefon pintar untuk pengesanan glukosa masih belum dikaji sepenuhnya. Bagi mengatasi permasalahan ini, sebuah prototaip refraktometer laser berasaskan telefon pintar secara tidak invasif telah dibangunkan untuk pemantauan glukosa secara berterusan untuk pesakit diabetes. Prototaip ini mengukur indeks refraktif air kencing dengan menganalisis kepanjangan laser yang direfraksikan. Saiz kepanjangan laser adalah berkorelasi dengan kepekatan glukosa darah untuk pesakit diabetes yang berpuasa. Prototaip yang dibangunkan ini menggunakan telefon pintar untuk menangkap imej dengan resolusi yang tinggi yang disebabkan oleh refleksi dalaman secara total menerusi batang rod akrilik dan pembiasan yang disebabkan oleh air kencing. Penilaian dilakukan melalui beberapa siri ujian kepekatan glukosa secara terkawal, tahap kekeruhan yang berbeza, isipadu sampel yang berbeza, dan tempoh jangka hayat sampel. Penilaian isipadu dan tempoh jangka hayat tidak memberi kesan terhadap keputusan ujian, manakala penilaian kekeruhan membuktikan bahawa prototaip yang dibangunkan terhad kepada tahap 57 unit kekeruhan nephelometrik (NTU) bagi sampel air kencing. Keputusan tahap glukosa puasa yang diukur dalam air kencing juga dibandingkan dengan keputusan makmal glukosa darah pesakit diabetes yang berpuasa dengan pekali korelasi sebanyak 0.89 dan sensitiviti sebanyak 4.8

mg/dL. Prototaip ini membolehkan pemantauan pemantauan glukosa secara berterusan untuk pesakit diabetes. Selain itu, prototaip yang dibangunkan ini agak berpatutan dari segi kos dan boleh digunakan untuk aplikasi teleperubatan. Ini seterusnya dapat membuka jalan kepada pengesanan glukosa secara klinikal untuk pesakit diabetes tanpa memerlukan cucukan jari secara invasif bagi mendapatkan sampel darah.

Kata kunci: *Pengukuran optik laser, refraktometer, tidak invasif, pemantauan glukosa, telefon pintar*

TABLE OF CONTENTS

		Page
DECLARATION		**i**
ACKNOWLEDGEMENT		**ii**
ABSTRACT		**iii**
ABSTRAK		**iv**
TABLE OF CONTENTS		**vi**
LIST OF TABLES		**x**
LIST OF FIGURES		**xi**
LIST OF ABBREVIATIONS		**xii**
CHAPTER 1	**INTRODUCTION**	**1**
1.1	Study background	1
1.2	Problem statement	3
1.3	Scope of study	4
1.4	Research questions	4
1.5	Hypothesis	5
1.6	Objectives	5
CHAPTER 2	**LITERATURE REVIEW**	**6**
2.1	Overview	6

2.2 Current semi-invasive and non-invasive glucose measuring devices 6

2.3 Invasive glucose monitoring 7

2.4 Semi-invasive glucose monitoring 7

2.5 Non-invasive glucose monitoring 8

2.5.1 Urinalysis 8

2.5.2 Colorimetry 8

2.5.3 Biosensors 10

2.5.4 Microwave sensor 12

2.5.5 Raman spectroscopy 14

2.5.6 Capacitance spectroscopy 17

2.5.7 Near-infrared spectroscopy 18

2.5.8 Mid-infrared spectroscopy 19

2.5.9 Fluorescence spectroscopy 20

2.5.10 Electrochemical 21

2.6 Section summary 23

2.7 Research gap 26

CHAPTER 3 METHODOLOGY 27

3.1 Overview 27

3.2 Theory 28

3.3 Experimental setup 31

3.4 Materials and Samples 33

3.4.1 Glucose sample preparation 35

3.4.2 Actual urine 37

3.4.3 Blood report 37

3.5 Assessing the effects of urine variation on measurement 38

3.5.1 Different sample volumes 38

3.5.2 Different sample turbidity 39

3.5.3 Shelf-life 41

3.5.4 Sensitivity, specificity, positive predictive values (PPV) and negative predictive values (NPV) 41

CHAPTER 4 RESULTS AND DISCUSSION 44

4.1 Overview 44

4.2 Preliminary tests 44

4.3 Assessing the effects of urine variation on measurement 46

4.3.1 Effects of varying volume on measurement 46

4.3.2 Effects of varying turbidity on measurement 48

4.3.3 Effects of shelf-life on measurement 51

4.4 Actual urine 53

4.4.1 Comparison with fasting glucose levels 54

4.5 Sensitivity, specificity, positive predictive values and negative predictive values 57

CHAPTER 5 CONCLUSION AND RECOMMENDATIONS **59**

5.1 Conclusion 59

5.2 Recommendations 60

REFERENCES **61**

APPENDICES **71**

LIST OF TABLES

		Page
Table 2.1:	Current commercial glucose monitoring devices	7
Table 2.2:	Peaks of Raman spectroscopy of urine and their assignments (Zou et al. (2016)	15
Table 2.3:	Peaks of Raman spectroscopy of micro vessels and their assignments (Li et al. (2019)	16
Table 2.4:	Summary of non-invasive detection methods, media of detection, sensitivity and correlation coefficients	24
Table 3.1:	Samples prepared for preliminary testing using water and glucose powder with varying weights for varying glucose concentrations	35
Table 3.2:	Varying glucose concentration and varying volumes used for effects of volume on performance of smartphone-based laser refractometer	39
Table 3.3:	Varying coffee powder weight used for measurement of turbidity, NTU	40
Table 3.4:	Test results of using smartphone-based laser refractometer to determine true positive, true negative, false positive and false negative	42
Table 4.1:	Results of varying volume and varying glucose levels	46
Table 4.2:	Results of Nephelometer and corresponding smartphone-based laser refractometer results	49
Table 4.3:	Smartphone-based laser refractometer results after 5 hours, 1 day and 2 days of sample acquired on 2nd and 23rd August 2024	52
Table 4.4:	Comparison of previous urinalysis methods for glucose sensing	57
Table 4.5:	True positive (TP), true negative (TN), false positive (FP) and false negative (FN) results from smartphone-based laser refractometer	58

LIST OF FIGURES

		Page
Figure 2.1:	Overview of types of glucose measurement methods	6
Figure 3.1:	Flowchart of smartphone-based laser refractometer development	28
Figure 3.2:	Front view of (a) Sample A with lower glucose concentration, (b) Sample B with higher glucose concentration. Side view of (c) Sample A with lower glucose concentration, (d) Sample B with higher glucose concentration. (e) Detailed front view of Sample B with higher glucose concentration. Images drawn not to scale	30
Figure 3.3:	Smartphone-based laser refractometer design (a) in isometric and, (b) side view in AutoCAD. (c) 3D printed smartphone-based laser refractometer	32
Figure 3.4:	Top view of measured laser line using prototype (a) with ambient lighting (b) controlled lighting	33
Figure 3.5:	Blood report of patient	38
Figure 4.1:	Smartphone-based laser refractometer glucose concentration (mg/dL) vs glucose concentration (mg/dL)	45
Figure 4.2:	Glucose concentration (mg/dL) vs refractive index, n	45
Figure 4.3:	Planar position of measured laser line in (a) 10 mℓ of 100 mg/dL, (b) 30 mℓ of 100 mg/dL, and (c) 50 mℓ of 100 mg/dL glucose solutions	47
Figure 4.4:	Detailed side view of sample with higher glucose concentration	48
Figure 4.5:	Image of sample with turbidity of (a) 0 NTU, (b) 57 NTU, and (c) 106 NTU	49
Figure 4.6:	Intensity profile comparisons of 0 NTU with (a) 26 NTU, (b) 57 NTU, (c) 75 NTU, and (d) 106 NTU	51
Figure 4.7:	Smartphone-based laser refractometer (mg/dL) vs fasting glucose concentrations (mg/dL)	56

LIST OF ABBREVIATIONS

AgNC	Silver nanocube
APSB	Advanced Pathology Sdn. Bhd.
AuNPs	Gold nanoparticles
CNPs	Carbon nanoparticles
FN	False negative
FP	False positive
GOx	Glucose oxidase
H_2O_2	Hydrogen peroxide
MIR	Mid-infrared
NIR	Near-infrared
NPV	Negative predictive values
NTU	Nephelometric turbidity units
PBP	Puncak Borneo Prison
PPV	Positive predictive values
TN	True negative
TP	True positive

CHAPTER 1

INTRODUCTION

1.1 Study background

Diabetes mellitus is a well-known chronic metabolic disorder that is caused by an increase in plasma glucose levels. This happens due to lack of production or action of insulin in the body. Diabetes mellitus can be mainly categorized into three types namely Type 1, Type 2 and gestational (Lovic et al., 2020). Type 1 diabetes mellitus (T1DM) happens because pancreatic β-cells are destroyed by the autoimmune system. T1DM is believed to be mainly genetic which explains why it can occur from a young age known as "childhood-onset diabetes" (Egan et al., 2019; Lovic et al., 2020). Type 2 diabetes mellitus (T2DM) on the other hand is the more common of the three types of diabetes mellitus. T2DM is developed in a person because of defective insulin secretion and unresponsiveness of the body to insulin. This can happen due to lack of a healthy lifestyle and diet (Galicia-Garcia et al., 2020). Gestational diabetes happens during pregnancy due to carbohydrate intolerance. It is very common and will most likely resolve post-delivery. However, mothers are usually assessed after birth since they are at risk of T2DM (Sweeting et al., 2022).

Estimates predict for the year 2045 it is expected that the number of diabetes mellitus patients will reach a staggering 629 million (Chen et al., 2021). It is also estimated that 90% of the current number of diabetic patients are of T2DM and the problem with diabetes arises when 50% of the patients are undiagnosed (Chen et al., 2021). This becomes extremely life-threatening when the patient remains unaware of their condition and continues to lead an unhealthy lifestyle especially in rural areas where they have no access to proper healthcare. When a person is diagnosed with diabetes, it is crucial for them to monitor their glucose

levels. A certain level of glucose in the body should be maintained to avoid complications such as kidney damage, stroke, and heart disease (Kaul et al., 2013).

Diabetes monitoring can be done frequently through non-invasive methods which include microwaves, spectroscopy, electrochemical, fluorescence and urinalysis. According to studies of Cebedio et al. (2020); Hanna et al. (2020); Hanna et al. (2022); Omer et al. (2020) and Tanaka et al. (2020), microwaves can be used to measure the permittivity of different body parts. Spectroscopy includes Raman, capacitance, infrared and fluorescence. Raman spectroscopy by Bezuglyi et al. (2018); Li et al. (2019); Lundsgaard-Nielsen et al. (2018) and Zou et al. (2016), requires a Raman spectrometer to measure the spectra obtained from different parts of the body, analyzing different peaks which are correlated with glucose levels. According to Dutta et al. (2019), Rassel et al. (2023), and Yao et al. (2021), capacitance spectroscopy measures the different capacitance of body parts or samples by placing them between two sensors connected to a multimeter. Infrared spectroscopy uses infrared to measure the absorbance of the infrared after going through a sample. Although these methods result in high correlation coefficient, the devices used are highly complex. For both electrochemical and fluorescence spectroscopy, these methods utilize catalysts which react with glucose. According to Lin et al. (2022); Lipani et al. (2018); Ribet et al. (2018); Sempionatto et al. (2019) and Sempionatto et al. (2021), electrochemical methods use glucose oxidase with glucose to produce hydrogen peroxidase (H_2O_2) which yield electrical energy that correlates with glucose levels in the sample (interstitial fluid). Fluorescence on the other hand uses catalysts such as silver nanocube (AgNC) (Jiang et al. (2019), carbon nanoparticles (CNPs) (Lu et al. (2021) and palladium-based nanostructures (Nie et al. (2020) which will react with glucose. The resulting fluorescence of these reactions and catalysts are measured by a spectrophotometer.

Urinalysis includes colorimetry and biosensors for measurement of glucose, protein, creatine, albumin and more. For colorimetric urinalysis, Pohanka et al. (2024) and Tohl et al. (2024) analyzes the changes in colour in test strips, while Feng et al. (2023) and Firdaus et al. (2022) analyzed the colorimetry of gold nanoparticles. Work reported by Tohl et al. (2024) measured creatine and albumin by change in colours of test strips with a limit of detection 1 mg/dL with a correlation coefficient of 0.73. Stability was an issue because the results of test strip colours vary due to urine colour variation. Similarly Pohanka et al. (2024) proposed a simpler setup to measure colorimetry of test strips for glucose detection with a limit of detection of 1.98 mg/dL. However, an incubation of 60 seconds of the samples is necessary for optimum results. Work reported by Feng et al. (2023) studied the colorimetry of gold nanoparticles (AuNPs) producing highly sensitive results of 0.0002 - 0.0018 mg/dL for glucose detection but at the expense of slow detection rate (190 seconds) and expensive biosensors fabrication. Work by Firdaus et al. (2022) also did a study on AuNPs colorimetry for glucose detection with a high sensitivity of 0.00008 mg/dL but requires optimum conditions of the samples (pH = 7, temperature = 30 °C and incubation of 30 minutes) and complex and expensive biosensors fabrication.

1.2 Problem statement

The current methods for urinalysis using colorimetry and biosensors often rely on laboratory-based setups and are not user friendly, limiting their accessibility and practicality for continuous glucose monitoring (Feng et al., 2023; Firdaus et al., 2022; Hajimiri et al., 2023; Nguyen et al., 2023; Fenoy et al., 2022). Although colorimetry is inherently a non-invasive method, the results are qualitative in nature. It is important to obtain quantitative rather than qualitative results for diagnosing, monitoring and managing the disease to ensure proper medical care is addressed. Despite the promising potential of integrating smartphones

with laser-based refractometry for glucose detection, Diez Alvarez et al. (2023) reported that research in this area remains limited. This gap highlights the need for a portable, affordable, and user-friendly solution for non-invasive glucose monitoring, offering ease of use for patients managing diabetes. By implementing smartphones and refractometry, this approach provides a non-invasive and rapid method for glucose monitoring, offering significant advantages over conventional invasive methods and the complex non-invasive methods proposed in existing research.

1.3 Scope of study

i. The medium used for measuring glucose will be urine samples.

ii. The minimum sample size of 132 (Sadiq et al., 2024).

iii. The sample collected disregard the age, gender and diabetes status.

iv. The glucose measurement results will be correlated with glucose levels obtained from blood reports and glucometer reading supplied by the collaborators.

v. The mechanisms used for glucose measurement in urine are based on total internal reflection and law of refraction.

1.4 Research questions

i. How smartphone and laser can be combined to measure glucose levels in urine?

ii. What are the effects of volume variation, turbidity and shelf-life of urines on measurement results?

iii. What is the correlation between the measured refracted laser length and laboratory results of fasting glucose levels?

1.5 Hypothesis

i. A smartphone and laser, combined with optical-based refractometry, can be designed to measure the refractive index in urine, which correlates with blood glucose levels.

ii. The volume variation, turbidity and shelf-life of urines have no effect on the measurement results.

iii. The length of measured refracted laser length is inversely proportional with the laboratory results of fasting glucose levels.

1.6 Objectives

i. To design and fabricate a smartphone-based laser refractometer for non-intrusive measurement of glucose in urine.

ii. To assess the developed smartphone-based laser refractometer, accounting for variations in urine volume, turbidity, and shelf-life.

iii. To assess the efficacy of the smartphone-based laser refractometer for glucose measurement in urine with laboratory results.

CHAPTER 2

LITERATURE REVIEW

2.1 Overview

In the current innovation of biomedical development, there are three different types of glucose measurement methods i.e., invasive, semi-invasive and non-invasive (Figure 2.1). Invasive methods involve deep penetration (capillaries, veins or tissues) on parts of the body, to obtain samples for analysis. Semi-invasive methods, however, require only shallow penetration (dermal or subcutaneous layers) on parts of the body, causing less intrusion. Non-invasive methods go a step further by eliminating the need for any penetration of the body, significantly reducing both discomfort and potential harm to the patient.

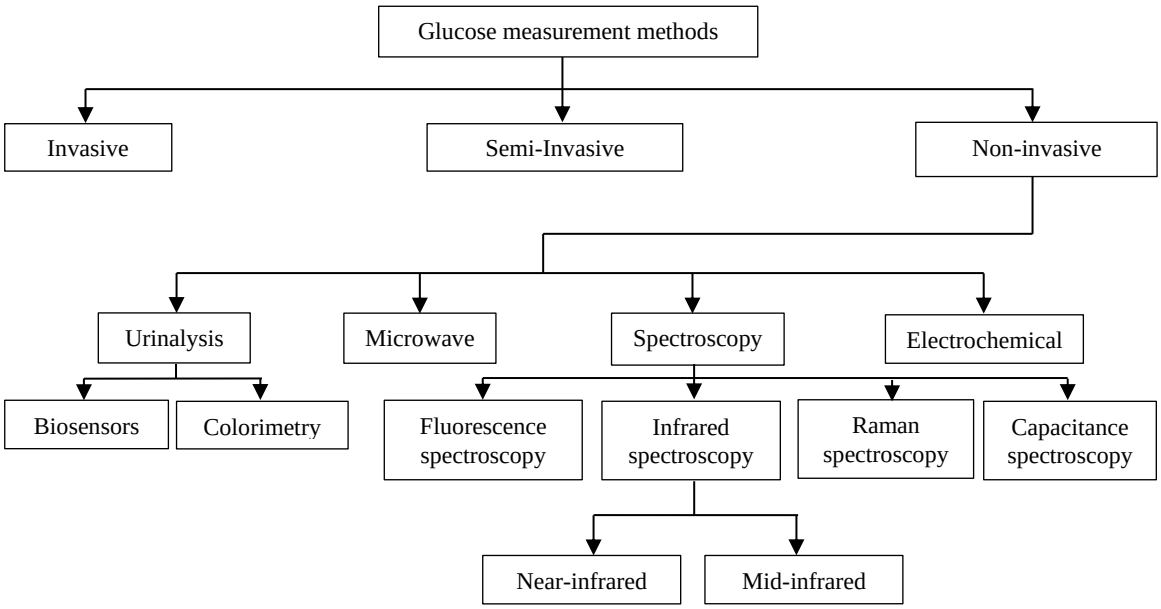

Figure 2.1: Overview of types of glucose measurement methods

2.2 Current semi-invasive and non-invasive glucose measuring devices

The current commercial semi-invasive and non-invasive glucose monitoring devices available in the market are as shown in Table 2.1. The apparent issue with these devices is

that technology uses patches which means patch life is a limitation which can last from one day up to 90 days. These patches can also be costly for the user in the long run.

Table 2.1: Current commercial glucose monitoring devices

Name	**Freestyle Libre (Abbott (2018)**	**Platinum G6 (Dexcom (2018a)**	**Platinum G5 (Dexcom (2018b)**	**Eversense (Senseonics (2018)**	**SugarBeat (Nemaura (2018)**
Manufacturer	Abbot	Dexcom	Dexcom	Senseonics	Nemaura Medical
Technology	Inserted sensor	Inserted sensor	Inserted sensor	Implanted sensor	Implanted sensor
Patch life	14 days	10 days	7 days	90 days	1 day
Accuracy	99%	-	97%	99.1%	95%
Device cost	RM 280.00	-	RM 2660.00	-	RM 168.00
Patch cost	RM 19.60	-	RM 40.88	-	RM 11.20

2.3 Invasive glucose monitoring

The current conventional glucometers are considered invasive since pricking is necessary for the user. Patients are required to prick their fingers to obtain blood which is applied to strips for the glucometer to read. Chemical reactions of the blood will then be converted to electrical energy to determine the blood glucose levels (Gonzales et al. (2019).

2.4 Semi-invasive glucose monitoring

Semi-invasive, or minimally invasive methods are similar to invasive methods as they also require the extraction of bodily fluids for analysis. Bollella et al. (2019) and

Chinnadayyala et al. (2021) both conducted experiments using highly porous microneedle-based electrodes. Bollella et al. (2019) conducted only in vitro testing which achieved a linearity range of 1.8-180 mg/dL with a processing time of two minutes. Whereas Chinnadayyala et al. (2021) used microneedles made of platinum black. In vitro tests were done which demonstrated a linearity range of 18-360 mg/dL and a processing time of two seconds. In this work, in vivo tests were conducted which showcased stability of up to seven days.

2.5 Non-invasive glucose monitoring

In the current state of non-invasive glucose monitoring studies, many methods are studied. Non-invasive methods can be divided into several main categories consisting of urinalysis, Raman spectroscopy, infrared spectroscopy, microwaves, capacitance spectroscopy, fluorescence and electrochemical.

2.5.1 Urinalysis

A well-known non-invasive method of glucose monitoring use the urine strips. Urine strips contain multiple chemical substances that will change colour when in contact with urine. Colours apparent on the strips are compared to a reference to determine the levels of different compositions found in urine such as glucose (Pighi et al. (2023).

2.5.2 Colorimetry

Tohl et al. (2024) approached this method using smartphones to analyze the colorimetry of the strips. The strips used in this study are One Step DUSTM 12AC. The camera used in this study is the Sony IMX219 camera module. The device uses a box with light sources and multiple reference points in order to calibrate. Once calibrated, the difference between colours of the test strips and reference colour blocks helps determine the

values of glucose, bilirubin, ketones, specific gravity, blood, pH, protein and much more. The result of the proposed device proved to have a correlation coefficient of 0.73 while visual assessment had a correlation coefficient of 0.63. It was found that the values obtained from the proposed method tend to be lower than their clinical values. Also, urine colour can affect the results of the test strips used, indicating a weakness in this method.

Pohanka et al. (2024) also used smartphones to analyze the colorimetry of test strips. In this research, standard urine strips (DekaPhan Leuco) were used. As for the camera, the proposed method used a Redmi Note 11 Pro with settings of 1× zoom, automatic flash, and automatic white balance. The images obtained are 8bit jpeg with 5 image acquisitions for each sample. The colours in the images are then analyzed using GIMP 2.10.34. The results obtained in terms of glucose were split into three (red, green and blue). For red, the coefficient of determination was $R^2 = 0.995$ while as for green and blue it was $R^2 = 0.991$ and $R^2 = 0.973$ respectively. Similar to Tohl et al. (2024), this method used test strips which means that urine colour can affect the results of the system.

As for Feng et al. (2023), artificial intelligence was utilized to analyze colour changes while being able to deter environmental factors such as ambient light. In this study, AuNPs coupled with Benedict's reagent were used. The changes in colour are analyzed via an android application using a smartphone. The results of this study had a coefficient correlation of $R^2 = 0.876$. The proposed method however had a slow detection rate of 190 seconds and expensive biosensor fabrication.

Firdaus et al. (2022) also used AuNPs for detection of glucose. It was evident that the blue hue of AuNPs changed to red with the introduction of glucose. An application for smartphone was also developed to detect these changes in the solution. As a reference,

ultraviolet-visible spectrometry was also done alongside the app for comparison. Results from this study had a sensitivity of 0.00008 mg/dL and a correlation coefficient $R^2 = 0.998$. This method was difficult to replicate because the urine samples must meet certain parameters (pH = 7, temperature = 30 °C and an incubation time of 30 minutes) and also had expensive biosensor fabrication.

While studies in colorimetry transform the qualitative nature into a quantitative one, the methods mentioned above can be affected by the colour variability of urine, as reported by Tohl et al. (2024) and Pohanka et al. (2024). Urine colour variation can be caused by hydration, diet, medication and health condition (Skrajnowska et al. (2024)). This poses as a limitation because the user must meet certain conditions to achieve accuracy and consistency of their proposed methods. and In comparison, Feng et al. (2023) achieved a detection rate of 190 seconds, whereas Firdaus et al. (2022) reported an incubation time of 30 minutes.

2.5.3 Biosensors

Hajimiri et al. (2023) however approached urinalysis by means of biosensors. Tablet based sensors were developed consisting of glucose oxidase (GOx) and horseradish peroxidase encapsulated in dextran. The tablets are incubated together with urine and a phosphate buffer solution. The purpose of the buffer solution is to dilute and adjust the pH value of the urine samples. After five minutes of incubation, the colour of the solution is observed where urine with glucose will produce a blue solution. Ultraviolet-visible spectrometer is used to measure the absorbance (at 652 nm) of the final blue solution which correlates with the glucose levels. Results showed a calibration curve of $R^2 = 0.9899$.

Similarly, the proposed method requires optimum conditions of the urine samples (pH = 7.4 and temperature = 60 °C and incubation time of five minutes).

Nguyen et al. (2023) had a similar approach but used zinc sulfide doped manganese encapsulated by chitosan. 1500 µL of 100 mg/L of the solution is placed in a cuvette where glucose solutions are later added. Glucose solutions are added with increments of 3.6 mg/dL. The final solution photoluminescence is measured using a spectrophotometer with a 10 nm slit. With the increase of glucose concentrations, it was found that the absorbance at 230 nm decrease with a coefficient correlation of R^2 = 0.993. Nguyen et al. (2023) further the research by adding phosphate buffered saline to the solution. This is expected to improve the study where it resulted in R^2 = 0.997. It is also noted that the absorbance of the solution with phosphate buffered saline was measured at 365 nm.

Fenoy et al. (2022) used graphene field-effect transistors (gFETs) alongside a multi amino polymer to bind with GOx. When samples induced with glucose were introduced to the solution, it was noticed that the current of the transistors dropped. The changes in this transistor correlate with the glucose levels in the samples. This study achieved a correlation of R^2 = 0.998 at the expense of detection rate of 190 seconds and complex biosensor fabrication process.

Similar to colorimetry, biosensors as a method require incubation time with the addition of expensive and complex fabrication of the said biosensors. This can be a challenge for the users especially if the application of glucose reading is for isolated areas or even for the average person. Additionally, biosensors often have a limited shelf-life which can further be a limitation for this method.

2.5.4 Microwave sensor

Cebedio et al. (2020) designed a non-invasive glucometer by means of a microwave sensor. The measurement of blood glucose levels in this study depends on the electromagnetic properties of blood, specifically permittivity. A resonator was found to be most suitable for measuring the permittivity of the blood which is correlated with blood glucose levels. In this study, the subject was ordered to place a finger on the resonator which is connected to a computer for further analysis. Results showed a correlation coefficient, $R^2 = 0.91$. The high sensitivity of the system was attributed to the considerably large contact volume and reduced with the decrease of contact volume due to lower interaction of the microwaves with the blood tissue.

Hanna et al. (2020) introduced a flexible sensor so that it is easier to fit to body parts such as the arm or legs. This would also allow more comfort and freedom of movement for the user. The system uses two electromagnetic sensors: first a multiband slot antenna and a multiband-reject filter. The microwaves from these sensors operate from 500 MHz up to 3 GHz. This makes it easier to reach veins, arteries, muscle, and fat tissues in the skin. Tests were done using fetal bovine serum and glucose solutions from 90 mg/dL to 126 mg/dL with increments of 10 mg/dL. Results from the antenna operating at 1.15 GHz were compared to a commercial glucometer to which the correlation of $R^2 = 0.98$ was achieved. While results from the flexible filter operating at 1.575 GHz achieved $R^2 = 0.95$. This study, however, was only done in vitro in fetal bovine serum rather than actual human subjects.

Following the earlier work, Hanna et al. (2022) further developed a continuous glucose measuring method wirelessly using flexible sensors operating at frequencies from 0.5 to 4 GHz to penetrate human tissues of the human leg. Reflected waves are then recorded

to determine the changes in terms of dielectric properties which correspond to the glucose levels in the blood. The final product was tested on animals and humans with an accuracy of 100% and 99.01% respectively.

Omer et al. (2020) also used microwave sensors for glucose monitoring. The design uses four complementary split ring resonators arranged on a thin sheet of FR4 dielectric substrate for the fingertips. The setup consists of two coaxial cables which are for transmitting and receiving. The setup is then connected to a radar board operating about 2.4 – 2.5 GHz in the Industrial, Scientific and Medical (ISM) band for transmission to a processing machine (i.e., laptop). Optimal results could only be achieved provided the user remain stationary throughout the measurement process to avoid the effects of vibration.

Tanaka et al. (2020) also performed photoacoustic spectroscopy. The proposed method was differential continuous wave photoacoustic spectroscopy which uses the amplitude modulation of dual wavelengths. Two lasers are set to turn on and off at the same frequency of 380 kHz but 180 degrees out of sync with each other. Wavelengths of 1382 and 1610 nm were used to ignore water. Alongside the proposed method, three conventional methods were also done for comparison. The correlation coefficient from this study was found to be from 0.58 to 0.80. This study was conducted on different parts of the body which led to an issue in accuracy depending on which part of the body was used. Different parts of the body introduce different perfusion rates causing discrepancy in the measurement errors.

Microwave face challenges due to the complexity of the human body. Studies such as Hanna et al. (2022) and Tanaka et al. (2020) proposed wearables, but these approaches demonstrated varying sensitivity and accuracy depending on the body part used. Additionally, these methods are limited by the requirement for minimal movement, this is to

maintain a stable signal to capture the data more accurately. This makes it necessary for subjects to remain stationary which is a significant inconvenience.

2.5.5 Raman spectroscopy

Bezuglyi et al. (2018) conducted a study using ellipsoidal reflectors. A device was designed using a laser diode, telescoping system, and prism. Peak values were apparent at wavelengths 960 to 990 nm. A finger is placed between the telescoping system and the prism where the laser on the finger will emit an optical radiation producing the back-scattered light from the prism which is collected by an ellipsoidal reflector for Raman spectroscopy analysis. While the study was done in vitro, biological challenges such as blood oxygen levels can affect the results of the proposed method.

Zou et al. (2016) used urine of the patients instead. Urine samples are placed in a dish where a 782 nm diode laser focuses on the sample. Urine samples are mixed with Ag colloids which proved to improve the Raman scattering. From this experiment the Raman spectra can visualise the different peaks at different ranges. It was observed that peaks at 725, 808, 1136 and 1350 cm^{-1} (see Table 2.2) were significantly higher in diabetes mellitus (DM) patients compared to non-DM patients. The results of this study achieved a sensitivity and specificity of 85% and 90.5% respectively with an R^2 of 0.836. While the claims of this method are low-cost, it requires complex fabrication of Ag colloids as biosensors.

Table 2.2: Peaks of Raman spectroscopy of urine and their assignments (Zou et al. (2016)

Peak position (cm^{-1})	**Assignments**
527	Cholesterol ester/nucleic acids
665	Uric acid
725	Adenin, coenzyme A
808	Albumin
889	D-galactosamine
1003	Phenylalanine
1136	Phenylalanine
1350	Guanine
1465	Tryptophan

Li et al. (2019) performed Raman spectroscopy of blood in vessels. A portable optical coherence tomography was used in this study which had a light source with a wavelength of 830 nm. Table 2.3 shows the peak position (cm^{-1}) and the corresponding components. The laser targets the nailfold of the subject at a depth of 200 µm. This study was performed on volunteers where R^2 of 0.97927 was obtained. The issue faced by the author was that no current was detected when the concentrations were less than 5.4 mg/dL. This method also requires 30 minutes of reading time to reach a higher and more significant peak value. The author also reported decline in performance after three months.

Table 2.3: Peaks of Raman spectroscopy of micro vessels and their assignments (Li et al. (2019)

Peak position (cm^{-1})		Assignments
Microvessles	**Blood**	
650	643	Ascorbic acid
758	752	Trp
837	827	Fructose
858	855	Tyr, lac
885	-	-
902	898	Tyr
945	940	Citric acid
978	971	Fibrin

Lundsgaard-Nielsen et al. (2018) developed a confocal Raman spectrometer that measures blood glucose through the human skin, specifically at the thumb. The setup uses a continuous-wave diode laser at 830 nm wavelengths. First, the laser is redirected to human skin via a dichroic mirror so that it is concentrated on the base of the thumb while the base of the thumb is placed on a 500 µm magnesium fluoride window. When this happens, the interaction creates a Rayleigh scattered light, broadband fluorescence background and molecule-specific Raman photons. All of these are redirected and will be collected by a spectrometer for further analysis. From several tests, it was found that 240-320 µm was the most suitable depth range as this had an accuracy of 93%. Similar to Li et al. (2019), the method has a reading time that could reach up to 45 minutes depending on which part of the body was used.

While Raman spectroscopy shows promise as a method of glucose monitoring, the spectrometer itself can be expensive and therefore confined to laboratory settings. Studies like Li et al. (2019) and Lundsgaard-Nielsen et al. (2018) also reported long reading times of 30 and 45 minutes respectively.

2.5.6 Capacitance spectroscopy

Rassel et al. (2023) used capacitance spectroscopy to determine varying glucose samples ranging from 5.6 to 33.3 mmol/L. Two copper plates sandwich the sample where one side uses a force-sensitive pressure sensor while the output current was monitored by a multimeter. The results from this study had a correlation coefficient of $R^2 = 0.96$. However, stability issues related to sweating of the skin, varying body temperatures, humidity, and corrosion of the copper plates over time were not addressed. It was also mentioned in the report that a decrease in capacitance was observed caused by ionic characteristics (dipole orientation and conduction) of the blood.

Dutta et al. (2019) proposed glucose monitoring using capacitance spectroscopy. A capacitive transducer is designed where it uses the tissue of the finger as the dielectric material. Like Rassel et al. (2023), it uses two capacitive sensors where one of the capacitors act as the sensing capacitor while the other act as a dummy capacitor using air as its dielectric. The results were compared with the conventional glucometer with errors of ±3.5%. The errors are attributed to physiological condition, body temperature and blood pressure, similarly as reported by Rassel et al. (2023). The author also reported difficulties with variables in the blood.

In a similar approach using capacitance spectroscopy, Yao et al. (2021) proposed a two-electrode wearable continuous blood glucose sensor. The electrode used were made of

graphene, carbon nanotubes and glucose oxidase (G/CNTs/GOx) for the acting electrode and graphene, carbon nanotubes, silver and silver chloride (G/CNTs/Ag/AgCl) as the counter electrode. The electrochemical activity of the materials was measured in an aqueous electrolyte solution. The cyclic volumetry was done from -0.3 V to 0.9 V at a scan rate of 0.1 V/s. This causes the skin to excrete interstitial fluid through a reverse iontophoresis process where the interstitial fluid is used to measure the glucose in the body. The results obtained from the electrodes had a linear correlation coefficient of R^2 = 0.9894 which matched very well with a conventional glucose meter with high sensitivity.

Capacitance method on the other hand faced challenges with the variables of the blood (such as ionic characteristics which affects the dipole orientation and conduction) as a medium as reported by Rassel et al. (2023) and Dutta et al. (2019).

2.5.7 Near-infrared spectroscopy

Saleh et al. (2018) designed a method using near-infrared (NIR) spectroscopy for glucose monitoring. A sample of water mixed with sugar is placed between two LEDs. A 1550 nm LED will transmit light while a photodiode with a range from 1700-700 nm will read the light. Glucose levels in the sample are correlated with the voltage levels read by photodiode. Samples are prepared ranging from 60 mg/dL up to 300 mg/dL with 10 mg/dL increments. This experimental setup results in 74% accuracy. This proposed method however requires a three-minute reading time to obtain approximately 175 – 185 for each sample. The study was also done only in vitro.

Rachim et al. (2019) established a method of glucose monitoring using visible near-infrared (Vis-NIR). The study uses an LED with wavelength of 1400-2000 nm for the first overtone band and 780-1400 nm for the second overtone band. The reason for using multiple

LEDs is that different wavelengths can penetrate different layers of the skin, producing multiple spectra for analysis. The results of the study achieved a coefficient correlation, R^2 = 0.86. The study, however, was done in an optimum environment and conditions where the user is to remain stationary

Jain et al. (2019) proposed a NIR spectroscopy together with Huber's regression model to help improve the accuracy of the results. The setup consisted of two wavelengths at 940 nm and 1300 nm. The wavelength of 940 nm is used for both absorbance and reflectance spectroscopy while 1300 nm is used for only absorbance spectroscopy. For absorbance spectroscopy, the finger or earlobe sits between an infrared emitter and an infrared detector. As for reflectance spectroscopy, the infrared emitter and detector is one device. The correlation coefficient, R^2 was improved to 0.9084 after post-processing using Huber's method. The overall accuracy was found to be 94-95% of the predicted blood glucose levels. This study also faced stability issues with the variables in blood specifically blood pressure.

Alam et al. (2020) proposed using NIR and a photodiode sensor. The NIR used wavelengths from 1700-800 nm. After going through a fingertip, a photodiode of 1550 nm wavelength receives the transmitted NIR waves. The waves are converted to electrical energy which will run through a microcontroller to determine the glucose value. The results show an accuracy of 94.32% from 20 individuals.

2.5.8 Mid-infrared spectroscopy

Kasahara et al. (2018) developed a non-invasive glucose monitoring using a mid-infrared (MIR) absorption spectroscopy and using only three wavelengths from the obtained spectroscopy. The proposed method measures the absorbance of oral mucosa, using

attenuated total reflection prism. Hollow optical fibers act as a transmission line. Two Fourier transform infrared spectroscopy (FTIR) are used as MIR spectrometers. An attenuated total reflection prism made of zinc sulfide is placed into the patient's mouth between upper and lower lips. The absorbance of oral mucosa is measured by patient's propagating radiation. Wavelengths in the region from 1200 to 980 cm^{-1} were obtained at every 2 cm^{-1} to determine the most appropriate wavelengths which were 1050, 1070 and 1100 cm^{-1}.

Sim et al. (2018) proposed MIR photoacoustic spectroscopy which ignores skin secretions which was a well-known problem for photoacoustic spectroscopy. A high energy laser (laser width of 90 μm and repetition rate of 47.5 kHz) illuminates the skin which will result in thermal expansion, hence generating an acoustic wave. An image is taken of the fingertip during illumination for spectra analysis. Peaks were apparent at 1070, 1105, and 1140 cm^{-1}.

A key limitation of infrared spectroscopy for glucose monitoring is the lack of standardization in the wavelengths used. Different studies propose varying optimal wavelengths based on sample type and device used. This makes it difficult to reproduce and compare results.

2.5.9 Fluorescence spectroscopy

Jiang et al. (2019) proposed a non-invasive glucose monitoring by fluorescence technique. In the study, a signal amplification strategy based on AgNC, GOx and silver fluorescence probe is proposed. When the AgNC reacts with H_2O_2, it is oxidized into Ag+. H_2O_2 on the other hand is a product of glucose that has been oxidized by GOx. Ag+ will enhance the red fluorescence in which the fluorescence spectra will be measured by

fluorescence spectrophotometer. This study, however, was only done in vitro and requires a complex fabrication process of the AgNC all while having an incubation time of two hours.

Lu et al. (2021) also worked with fluorescence for glucose monitoring. In this study, the fluorescence of functionalized CNPs is affected by glucose. When glucose interacts with CNPs, it will enhance the fluorescence of the CNPs. Based on the fluorescence spectra obtained, wavelength of 420 nm was found to be the most reactive to glucose. The results from this experiment came out with a correlation coefficient of R^2 = 0.9818. Although showing good outcome, this method requires a very long incubation time of five hours.

Nie et al. (2020) employed fluorescence as a method for glucose monitoring that uses palladium-based nanostructures instead of CNPs used by Lu et al. (2021). Similar to other studies, the detection is based on the reaction occurring when palladium-based nanostructures are in contact with H_2O_2, turning the solution bluer as the level of H_2O_2 increases. Based on the spectra obtained, absorption at wavelength 652 nm is correlated with the glucose levels, with correlation coefficient, R^2 = 0.9928. Similar to Jiang et al. (2019), this proposed method requires an incubation time of two hours.

Fluorescence uses nanoparticles as reactants, because of this the fabrication is laboratory based and complex. The methods reported also require incubation time of two to five hours as reported above.

2.5.10 Electrochemical

Sempionatto et al. (2019) introduced eyeglasses that were capable of measuring alcohol, vitamin, and glucose levels from tears. The device has four key components; a fluidic device to obtain tears, electrochemical flow detector, wireless components and the

eyeglasses frames itself. To obtain some drop of tears, the device uses a super-hydrophilic polycarbonate which can absorb the tears from the eyes without the need for irritation or stimulation. The electrochemical sensors are an AOx-modified electrochemical flow detector. A biocatalytic conversion is done to the sample to produce gluconic acid and H_2O_2 using GOx found in the tears. The results of the H_2O_2 are selectively reduced by the Prussian Blue transducer.

Sempionatto et al. (2021) proposed a touch based electrochemical sensor from the fingertip for glucose monitoring. The device uses polyvinyl alcohol to absorb sweat from the fingertips by capillary pressure. The polyvinyl alcohol sits on top of the Prussian Blue transducer where there is an enzymatic layer in contact with the electrochemical biosensor. The electrochemical biosensor is used to evaluate the glucose levels in the sweat which correlates with glucose levels in blood. The results from this study showed a correlation coefficient, R^2 higher than 0.95. The method has a slow processing time of two minutes where the user has to touch the sensor for one minute then measured for another minute to obtain the final results.

Lin et al. (2022) developed a wearable hydrogel patch based on an electrochemical glucose sensor for natural sweat detection. The hydrogel patch acts as a medium to create a hydrophilic fluid to withdraw the sweat from the fingertip, back of hand or palm. From here, sweat is transferred to the electrochemical sensor via a nanostructure hybrid film. The electrochemical sensor consists of Prussian Blue and poly(3,4-ethylenedioxythiophene) nanocomposites (PB-PEDOT NC). Sweat obtained contains GOx which generates H_2O_2 that correlates with the glucose levels in sweat. The system was tested on three parts of the

subject which are the fingertips, palm and back of hand. The fingertip, palm and back of the hand showed a correlation coefficient of 0.88 0.70 and 0.90 respectively.

Lipani et al. (2018) and Ribet et al. (2018) developed a glucose monitoring devices using interstitial fluid from the skin. Lipani et al. (2018) obtained interstitial fluid by electroosmotic extraction whereas Ribet et al. (2018) used microneedles to probe the human skin. Interstitial fluid extracted is used with an electrochemical sensor to determine the glucose levels.

Studies based on electrochemical uses interstitial fluid to determine the glucose levels in the body. However, interstitial fluid as a medium can cause problems where the variability of the interstitial fluid can affect the accuracy of the results. An example of this was reported by Lin et al. (2022) where different parts of the body used had different correlation coefficients. A slow processing time could also be an issue for this method as reported by Sempionatto et al. (2021).

2.6 Section summary

Table 2.4 presents a summary of non-invasive detection methods, sample media, sensitivities, and correlation coefficients from previous studies reported in the literature. For non-invasive glucose monitoring methods, the studies show correlation coefficients ranging from 0.74 to a maximum of 0.99, indicating generally high accuracy across methods. Notably, most studies rely on body parts and interstitial fluid as sample media, with only a few utilizing urines as a detection medium.

Table 2.4: Summary of non-invasive detection methods, media of detection, sensitivity and correlation coefficients

Author	Method	Medium	Limit of detection, mg/dL	Correlation coefficient
Pohanka et al. (2024)	Colorimetry	Urine	1.98	0.998
Feng et al. (2023)	Colorimetry	Urine	0.0002	-
Firdaus et al. (2022)	Colorimetry	Urine	0.00008	0.99
Hajimiri et al. (2023)	Biosensors	Urine	0.103	0.99
Nguyen et al. (2023)	Biosensors	Urine	2.3	NA
Fenoy et al. (2022)	Biosensors	Urine	0.0007	0.95
Cebedio et al. (2020)	Microwaves	Finger	-	0.91
Hanna et al. (2022)	Microwaves	Legs	-	0.99
Omer et al. (2020)	Microwaves	-	-	-
Tanaka et al. (2020)	Microwaves	-	-	0.54-0.80
Bezuglyi et al. (2018)	Raman	Fingers	-	-
Zou et al. (2016)	Raman	Urine	-	0.84

Table 2.4: continued

Li et al. (2019)	Raman	Blood vessels in nailfold	-	0.98
Lundsgaard-Nielsen et al. (2018)	Raman	Thumb	-	0.93
Rassel et al. (2023)	Capacitance	-	-	0.96
Dutta et al. (2019)	Capacitance	Finger	-	-
Yao et al. (2021)	Capacitance	Interstitial fluid	-	0.99
Sim et al. (2018)	MIR	Skin	-	-
Sempionatto et al. (2019)	Electrochemical	Tears	-	-
Sempionatto et al. (2021)	Electrochemical	Sweat	-	0.95
Lipani et al. (2018)	Electrochemical	Interstitial fluid	-	-
Ribet et al. (2018)	Electrochemical	skin	-	-
Lin et al. (2022)	Electrochemical	Sweat	-	0.90
Karpova et al. (2019)	Electrochemical	Sweat	-	-
Jiang et al. (2019)	Fluorescence	-	-	-
Lu et al. (2021)	Fluorescence	-	-	0.98
Nie et al. (2020)	Fluorescence	-	-	0.99

2.7 Research gap

There are a number of studies exploring semi-invasive and non-invasive glucose monitoring through various methods, including spectroscopy (Raman, NIR, MIR, capacitance and fluorescence), microwave and electrochemical, as listed in Table 2.4. However, these studies primarily focus on interstitial measurements and specific body parts rather than urine, and few integrate smartphone technology. While urinalysis using colorimetry and biosensors have been investigated for glucose detection, these approaches often require laboratory-based setups and lack real-time, user-friendly integration. Research combining smartphone technology with laser-based refractometry for detecting glucose in urine remains limited, despite its potential to provide a portable, affordable, and user-friendly solution for non-invasive glucose monitoring.

CHAPTER 3

METHODOLOGY

3.1 Overview

In this section, the methodology in the setup to determine the glucose levels of patients accurately and consistently is discussed. Figure 3.1 shows the flowchart for the development of the smartphone-based laser refractometer and the appropriate assessments. Since the refractive index of urine is correlated with the patient's glucose levels, the theoretical framework was established to measure the effects of varying urine refractive index using a laser. This will ensure a pain free process of measuring the glucose levels when using urine. Preliminary tests are done with prepared glucose samples to determine the validity of the theory before advancing with actual urine samples. With success in preliminary tests, further assessments of the proposed method are made. Since this experiment uses urine, factors such as level, turbidity and shelf-life are considered to ensure consistency and accuracy of the proposed method. Finally, comparisons can be made with fasting glucose levels of urine samples to study the efficacy of the smartphone-based laser refractometer.

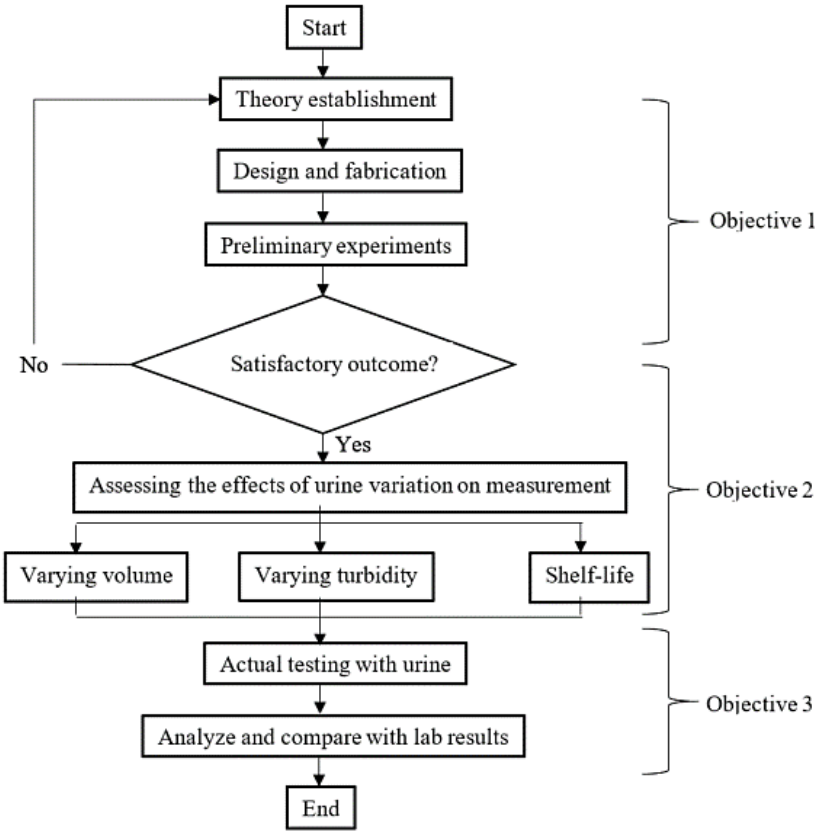

Figure 3.1: Flowchart of smartphone-based laser refractometer development

3.2 Theory

In this study the glucose concentration in urine will be determined as a function of the refractive index in the urine samples (Tamrin et al. (2018)). With the increase of glucose concentrations in urine, the refractive index will also increase (Kavitha et al. (2006)). As illustrated in Figure 3.2, a circular laser beam passing diametrically through an acrylic rod will be subjected to a total internal reflection. This causes the beam to be shaped in the form of elliptical beam. The size of the elliptical beam does vary with the diameter of the rod. Throughout the experiment the size of the rod remains the same. At the air-urine interface, the size of the elliptical beam (as a function of minor and major axes) will be varied depending on the refractive index of the sample.

$$\frac{n_{air}}{n_{urine}} = \frac{\sin\theta_r}{\sin\theta_i} \qquad \text{Equation 3.1}$$

Where n_{air} is refractive index of air, n_{urine} is refractive index of urine, θ_i is angle of incident and θ_r is angle of refraction. Assuming that n_{air} and θ_i are constants, θ_r is inversely proportional to n_{urine}. Hence, the length of refracted laser line is also inversely proportional to n_{urine}.

Assuming Sample B (Figure 3.2 (b)) has a higher refractive index than that of Sample A (Figure 3.2 (a)), the length (major axis) of the refracted elliptical beam in Sample B would be shorter than that of Sample A. On the other hand, the length (minor axis) is comparatively larger for Sample A. On this basis, the concentration of glucose in urine will be correlated with the refracted elliptical beam on major axis since the changes with respect to varying refractive indices is more pronounced than the latter.

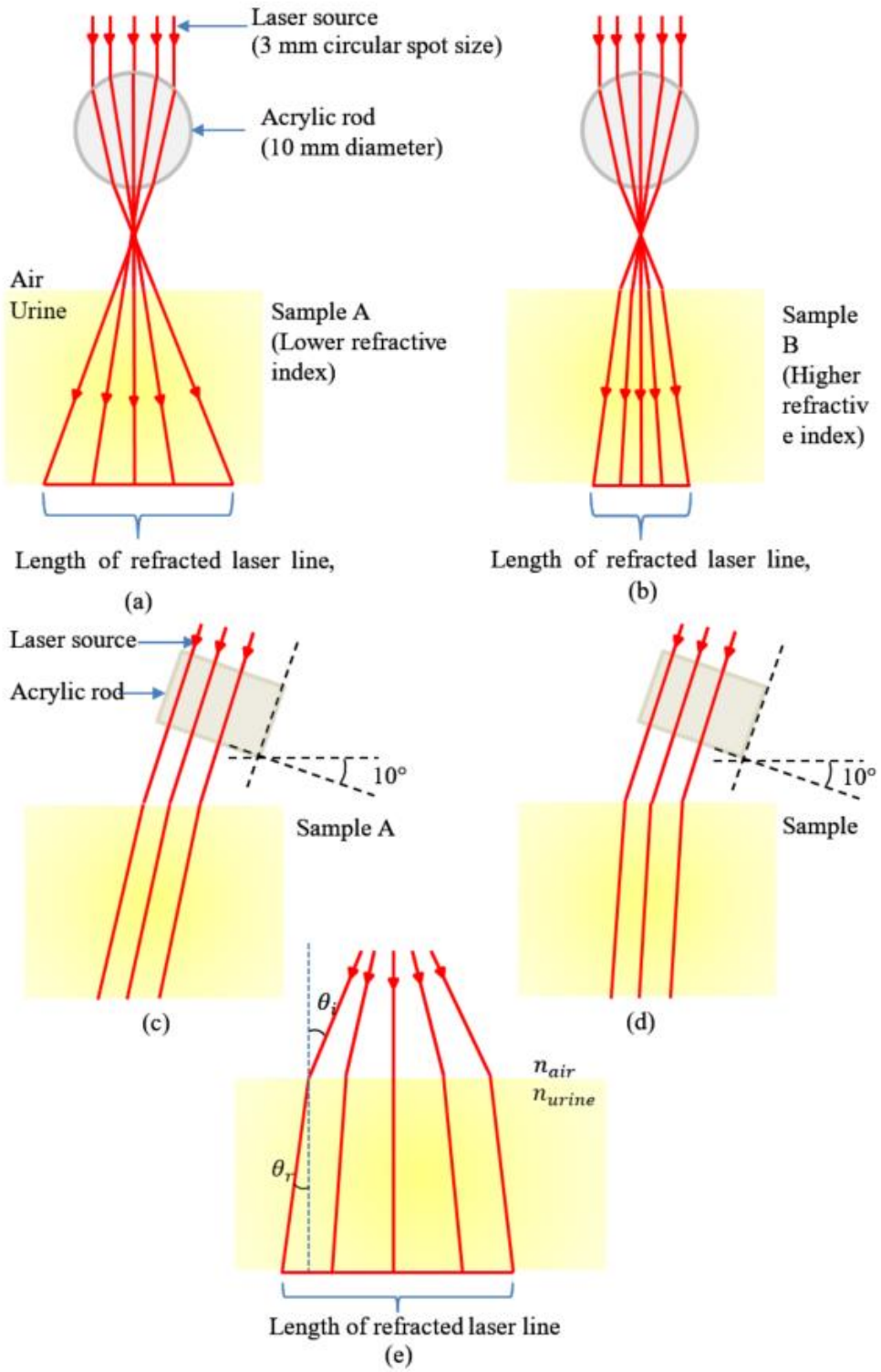

Figure 3.2: Front view of (a) Sample A with lower glucose concentration, (b) Sample B with higher glucose concentration. Side view of (c) Sample A with lower glucose concentration, (d) Sample B with higher glucose concentration. (e) Detailed front view of Sample B with higher glucose concentration. Images drawn not to scale

3.3 Experimental setup

The design of the smartphone-based laser refractometer as seen in Figure 3.3(a) and Figure 3.3(b) was done in AutoCAD. During the design phase, important factors were taken into account to ensure accurate and reliable results. It is important that the setup is robust because the whole concept depends on the stability of the parameters such as positioning of the smartphone lens, height between the smartphone lens and the subject, and the angle of the laser. The desired design was 3D printed (refer Figure 3.3(c)) using a 3D printer (Creality Ender V3). The material used was polylactic acid (PLA) and the printing was done with 20% infill. 20% was enough so that the printed product is solid and strong enough to withstand the weight of the smartphone on top of the setup without any vibration or instability.

The proposed design uses a smartphone, as for the current setup Apple iPhone 13 is used. However other phones can be used but with different prints of the top plate of the design to cater other phones. Additionally, the default camera app is not used because this did not allow full control of all the features of the camera such as the focus, ISO and shutter speed. Hence, an app called 'mcamera' is used to allow manual changing of these settings. To ensure accuracy and consistency, the settings of the camera must be consistent for every measurement. In all experiments, the focus was kept to 0.01 while the ISO was kept at 7.6K and the shutter speed to 1/16. This resulted in the best quality of the sample images.

The laser pointer is a crucial component of this setup to ensure consistency and accuracy. The laser pointer used was a rechargeable 5 mW laser pointer with wavelength of 650 nm, a beam spot size of 3 mm at standoff distance of 7 cm which was sufficient to cater for the measured length. To ensure consistency of the brightness of the laser, it was ensured that it was fully charged before measurements were made.

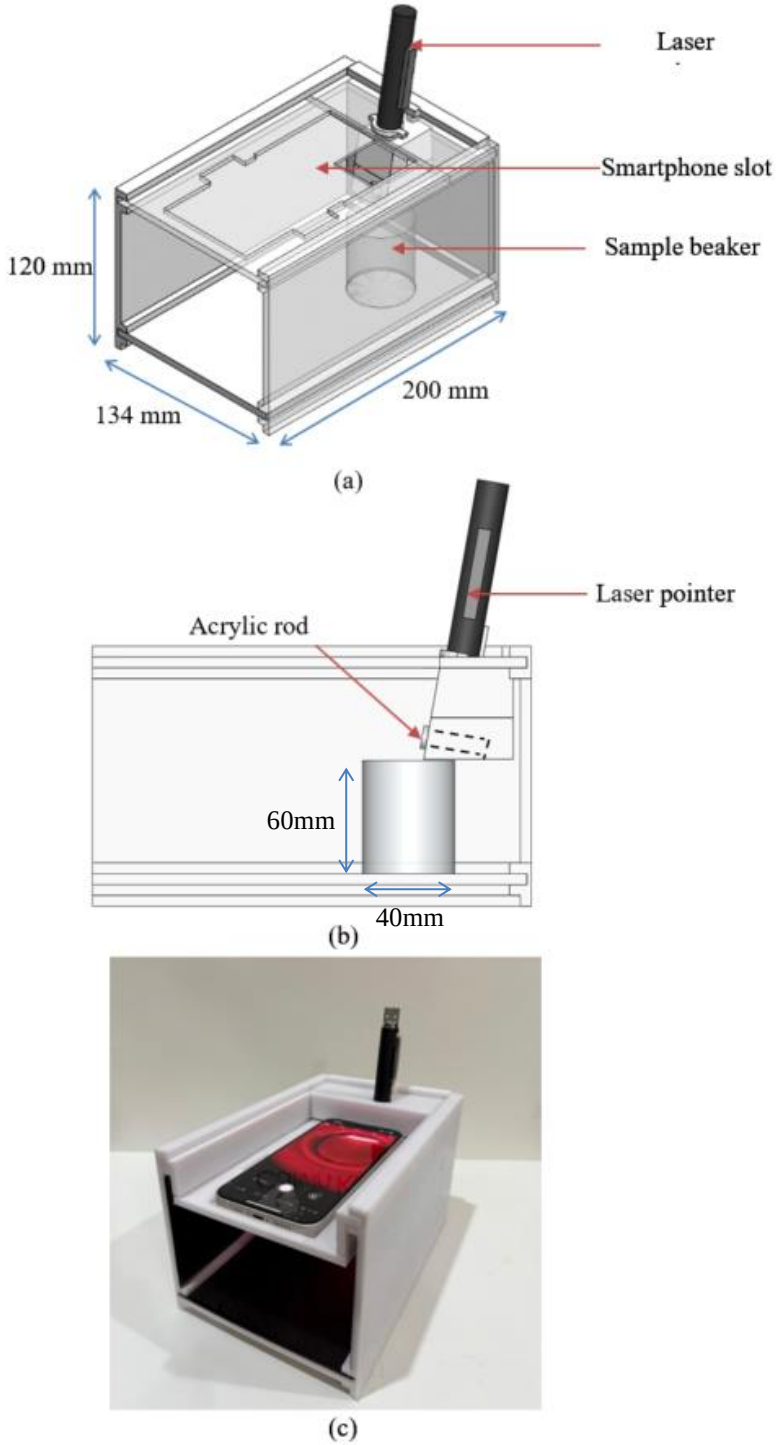

Figure 3.3: Smartphone-based laser refractometer design (a) in isometric and, (b) side view in AutoCAD. (c) 3D printed smartphone-based laser refractometer

Data for analysis is acquired from images captured using the smartphone-based laser refractometer (see Figure 3.4). As previously mentioned, the setup uses an iPhone 13 alongside a third-party app (mcamera) to ensure consistency of images taken. Images are

transferred to a laptop where the measurements of the laser line are done using paint (in pixels).

(a)

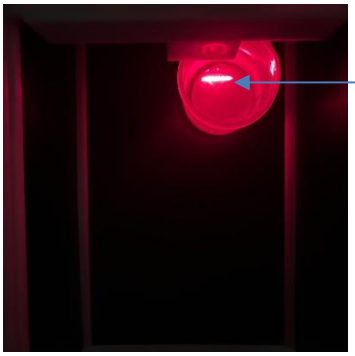

(b)

Figure 3.4: Top view of measured laser line using prototype (a) with ambient lighting (b) controlled lighting

3.4 Materials and Samples

This study involved secondary analysis of data collected by a collaborating laboratory, Advanced Pathology (M) Sdn. Bhd. (APSB) and Puncak Borneo Prison (PBP) obtained informed consent from all individual participants included in the study prior to data collection. All methods were carried out in accordance with relevant guidelines and

regulations. Ethical approval for the use of this data was obtained from *Mesyuarat Jawatankuasa Etika Perubatan Fakulti Perubatan dan Sains Kesihatan* no. 04/2018 on 11th December 2018.

There were 123 and 37 actual urine samples provided by Advanced Pathology (M) Sdn. Bhd. (APSB) and Puncak Borneo Prison (PBP), respectively. From APSB, urine samples, urinalysis and blood report were supplied. From PBP, they supply urine samples and glucometer reading. Samples from 37 patients at PBP were collected in the morning on the same day and their respective glucose levels were measured using a conventional glucometer (Contour Plus Elite by Contour Plus) to provide fasting glucose levels. Of the 123 samples from APSB, 56 fasting, 15 HbA1c and 52 both fasting and HbA1c samples were obtained.

Substances in the urine such as bilirubin, ketones and proteinuria can also alter the physical properties of the urine including the refractive index. To simply explain, bilirubin is a product of hemoglobin (red blood cells), ketones are from fats, proteinuria are from protein. All three of these can affect the refractive index of urine. However, urinalysis (dipstick) reports only a handful of urine samples with these substances present. Thus, samples with these substances present are disregarded.

The sample size for quantitative studies can be calculated using the following equation (Sadiq et al. (2024);

$$sample\ size, N = \frac{(Z)^2(Std\ Dev)^2}{(q)^2} \qquad \text{Equation 3.2}$$

Where Z is the critical value and a standard corresponding value of confidence, and q is the margin of error. For a 95% confidence level, which is the common used confidence

level, the critical value would be 1.96 (Sadiq et al. (2024). As for the standard deviation of this study it is 5.86 and the targeted margin of error is 1 mmol/L (18 mg/dL). Hence, the number of samples for this study can be calculated as follows;

$$sample\ size, N = \frac{(1.96)^2(5.86)^2}{(1)^2} = 132$$

Hence, the minimum number of samples required for this study is 132 samples.

3.4.1 Glucose sample preparation

Initially for the first preliminary experiment, a set of glucose solutions were prepared using water and glucose powder (Glucolin) ranging from 70 to 300 mg/dL (3.9 – 16.7 mmol/L) with increments of 10 mg/dL as seen in Table 3.1. Glucolin is a commercial brand energy drink made from dextrose monohydrate, a medicinal glucose which is used as a source of energy for the body. The solution was prepared by mixing 100 mℓ of water is added with 0.07 g (digital weighing scale with sensitivity of ±0.01 g) of glucose powder to obtain 70 mg/dL of glucose concentration. Then the steps are repeated to obtain up to 300 mg/dL glucose concentrations with increments of 10 mg/dL. It is also important to note that multiple pictures of the same sample are taken. This is to obtain the average length of the laser line. These are repeated for all readings.

Table 3.1: Samples prepared for preliminary testing using water and glucose powder with varying weights for varying glucose concentrations

Sample	Glucose powder (g)	Concentration (mg/dL)
1	0.07	70
2	0.08	80
3	0.09	90

Table 3.1: continued

4	0.10	100
5	0.11	110
6	0.12	120
7	0.13	130
8	0.14	140
9	0.15	150
10	0.16	160
11	0.17	170
12	0.18	180
13	0.19	190
14	0.20	200
15	0.21	210
16	0.22	220
17	0.23	230
18	0.24	240
19	0.25	250
20	0.26	260
21	0.27	270
22	0.28	280
23	0.29	290
24	0.30	300
23	0.29	290
24	0.30	300

3.4.2 Actual urine

As for urinalysis, “H-500 Urine Analyzer” by DIRUI is used. This machine uses a test strip with multiple reagent pads which will react with different substances in the urine. The change in colour of the reagent pads is determined by optical sensors which correlate with different parameters such as glucose, protein, pH value, specific gravity, and more.

3.4.3 Blood report

Figure 3.5 shows an example of a blood report provided by APSB. The lab sends their samples to a lab in Kuala Lumpur which uses a “Blood Biochemistry Analyzer” by Roche to analyze the blood samples. The machine mixes blood samples with reactive reagents for several detection methods. The methods used are photometric, turbidimetric and electrochemical detection. The machine is capable of determining multiple parameters such as bilirubin, creatinine, cholesterol, protein and glucose levels. This includes both fasting and HbA1c glucose levels as shown in Figure 3.5.

PATIENTS DETAILS

[redacted]

NRIC/PASSPORT : [redacted]
AGE : [redacted] SEX : [redacted] DOB : [redacted]
SPECIMEN COLLECTED : [redacted]
REPORT COMPLETED : [redacted]

DOCTOR DETAILS

[redacted]

KLINIK TANG

LOT 287, JALAN SATOK, 93400 KUCHING, SARAWAK

TEST NAME		RESULTS	UNITS	REF. RANGES
Diabetic studies				
HbA1c	糖化血紅蛋白	9.9 * H	%	(< 5.7)

HbA1c %	HbA1c mmol/mol	Diagnostic values of HBA1C for Diabetes Mellitus
< 5.7	< 39	Non-diabetic range
5.7 - 6.2	39 - 44	Indicative of pre-diabetes
>= 6.3	>= 45	Diabetic Level Monitoring values of HBA1C for known Diabetics General HbA1c target for known diabetics
<= 6.5	<= 48	Good diabetic control Individualised Hba1c target for known diabetics
6.0 - 6.5	<= 48	A: Tight target range for young, newly diagnosed patients without hypoglycaemia
7.1 - 8.0	54 - 64	B: Target range for diabetics with co-morbidities
6.6 - 7.0	49 - 53	C: Target range for all other individuals not in category A or B

Glucose	血糖	18.5 * H	mmol/L	(Fasting: 4.1 - 6.1)

Figure 3.5: Blood report of patient

3.5 Assessing the effects of urine variation on measurement

3.5.1 Different sample volumes

Since the experimental setup uses urine from patients, the volume of the urine was a concern for the setup. Since the volume of urine varies from different people, it was decided that volumetric assessment was necessary. As seen in Table 3.2, different volumes of samples (10 to 50 mℓ) were used to determine if this influenced the results. The samples were also done with increasing glucose levels for each volume to determine if the difference in volume would affect the consistency of the results. Assuming that it would not have any effects, the resulting length of the laser line would stay consistent for each volume.

Table 3.2: Varying glucose concentration and varying volumes used for effects of volume on performance of smartphone-based laser refractometer

Volume (mℓ)	**Concentration of prepared glucose solution**		
	100 (mg/dℓ)	200 (mg/dℓ)	300 (mg/dℓ)
10			
20			
30			
40			
50			
Average			
Std dev			

3.5.2 Different sample turbidity

Another factor that drew attention was the variation in colour and turbidity among different urine samples. Therefore, this test was necessary to determine if the colour and clarity of the samples affect the accuracy of the results. Since the proposed method relies on the refractive index, colour will not affect the results. In contrast, turbidity could influence the measurements. Unlike colorimetry, where colour can significantly impact the results, turbidity does not pose the same challenge in refractive index-based methods. Therefore, it is crucial to evaluate the impact of turbidity on the proposed device, rather than focusing on the effect of colour.

In this test, food grade coffee powder was used to vary the turbidity of the samples. Coffee powder was used to provide a cost effective and better reproductivity of the different

turbidity levels to better understand the effects of different turbidity to the proposed device. Samples are prepared using 2 ℓ of water and 0.25 g increments of coffee powder as seen in Table 3.3. Then the samples undergo a nephelometer to determine the NTU. This will determine up to which NTU level the proposed prototype would still be able to measure the glucose levels. The NTU of the coffee samples were measured using a calibrated nephelometer (Hach DR900).

After the turbidity of the samples are determined, the samples are used with the smartphone-based laser refractometer to determine up to which NTU the proposed prototype can still perform well. The glucose concentration is kept as a controlled variable in this section at 0 mg/dL.

Table 3.3: Varying coffee powder weight used for measurement of turbidity, NTU

Coffee powder (g)	Nephelometric turbidity unit (NTU)
0.00	0
0.25	26
0.50	57
0.75	75
1.00	106
1.25	131
1.50	148
1.75	179
2.00	190
2.25	228

3.5.3 Shelf-life

To ensure that the shelf-life of the samples would not affect the results, this assessment determine the outcome if the samples were read at different times. Samples are used with the proposed refractometer on the day of acquisition, after 1 day and after 2 days (Firdaus et al. (2022). Oxidization of the urine samples can be decelerated by keeping the samples around 4°C, using airtight containers and adding chemical preservatives. Chemical and bacteria activities are reduced drastically at 4°C. Samples are kept in airtight screw containers in refrigerators (1.7°C to 3.3°C). Storing them at a freezing point is not advisable as this would alter the chemical composition of the urine samples. Oxidization is to be avoided because it can affect the chemical, biological and physical (including refractive index) properties of the urine (Gharsallah et al. (2018). Samples from APSB are acquired on a weekly basis to avoid oxidized urine. The samples are also kept in airtight screw containers in refrigerators. For this reason, by keeping the samples in the above parameters, measurements will be taken 4 hours, 1 day and 2 days after acquisition.

3.5.4 Sensitivity, specificity, positive predictive values (PPV) and negative predictive values (NPV)

Table 3.4 demonstrates how to determine true positive (TP), false positive (FP), false negative (FN) and true negative (TN). True positive and true negative dictates that the prototype successfully determined that the patient does or does not have the disease. Whereas false positive and false negative dictates that the prototype failed to determine whether the patient does or does not have the disease.

Table 3.4: Test results of using smartphone-based laser refractometer to determine true positive, true negative, false positive and false negative

Test results	**Diabetes**	
	Has disease	**No disease**
+	True positive	False positive
-	False negative	True negative

According to Monaghan et al. (2021) sensitivity indicates how well an instrument dictates whether the subjects are truly positive. As for specificity, this indicates how well an instrument dictates whether the subjects are truly negative. PPV on the other hand determines the probability of a subject is positive when tested positive and vice versa for NPV.

To calculate the sensitivity, specificity, PPV and NPV of the instrument, the following equations are used (Monaghan et al. (2021);

$$Sensitivity = \frac{TP}{TP + FN} \times 100\% \qquad \text{Equation 3.5}$$

$$Specificity = \frac{TN}{FP + TN} \times 100\% \qquad \text{Equation 3.6}$$

$$PPV = \frac{TP}{TP + FP} \times 100\% \qquad \text{Equation 3.7}$$

$$NPV = \frac{FN}{FN + TN} \times 100\% \qquad \text{Equation 3.8}$$

In this study, glucose levels that are 130 mg/dL and above will be defined as positive results.

CHAPTER 4

RESULTS AND DISCUSSION

4.1 Overview

In this section, results of the preliminary test using the smartphone-based laser refractometer are showcased using samples prepared with glucose powder. Further assessments are done using the smartphone-based laser refractometer with respect to volumetric, turbidity and shelf-life assessments. For volumetric assessment, tests are conducted using different volumes of samples with concentrations as a controlled variable. Similarly for turbidity assessment the concentrations are a controlled variable while different turbidites are used to study the performance of the proposed method. As for shelf-life assessment, the smartphone-based laser refractometer was used on the same samples for in a span of three days to study the effects over time. Finally, actual urine samples are used to study the efficacy of the proposed method by comparing the results of the proposed method and the respective fasting glucose levels of the urine samples.

4.2 Preliminary tests

As mentioned in the previous chapter, preliminary tests are done using glucose samples prepared by adding glucose powder (Glucolin) with water. Samples used ranged from 70 to 300 mg/dL. The results proved the relationship between the glucose concentration and the length of the laser line to be inversely proportional to each other. Referring to Figure 4.1, the correlation coefficient of the proposed method and the glucose samples were R^2 = 0.8871 with a limit of detection of 1.4236 mg/dL. Measurements of the refractive index of the glucose samples are done by measuring a refracted laser line in the prepared glucose samples. The average angle is done with three images acquired for each glucose

concentration. This proved that the higher the concentration of glucose, the higher the refractive index of the sample (refer Figure 4.2).

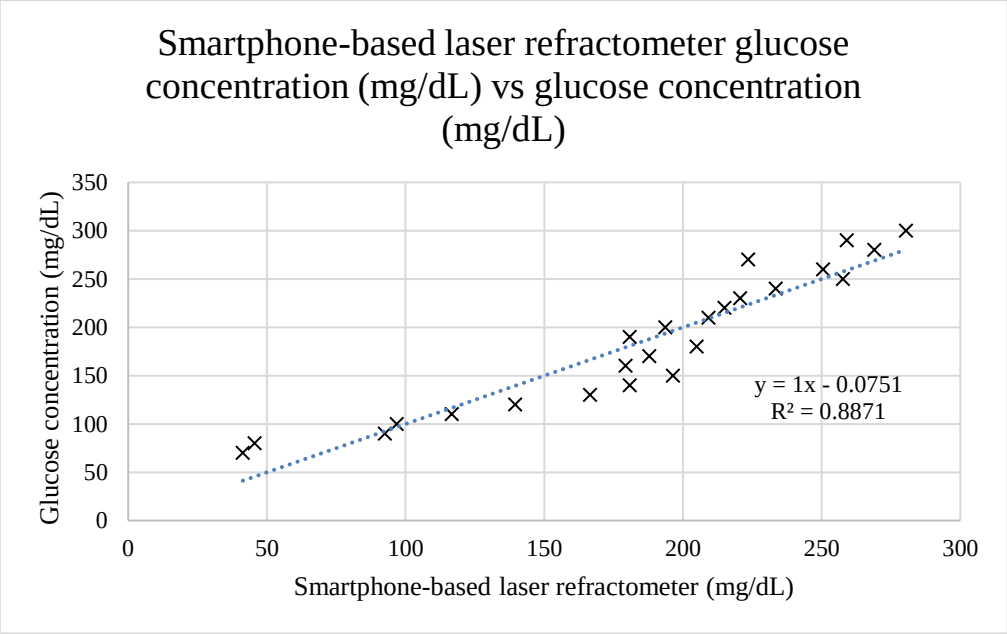

Figure 4.1: Smartphone-based laser refractometer glucose concentration (mg/dL) vs glucose concentration (mg/dL)

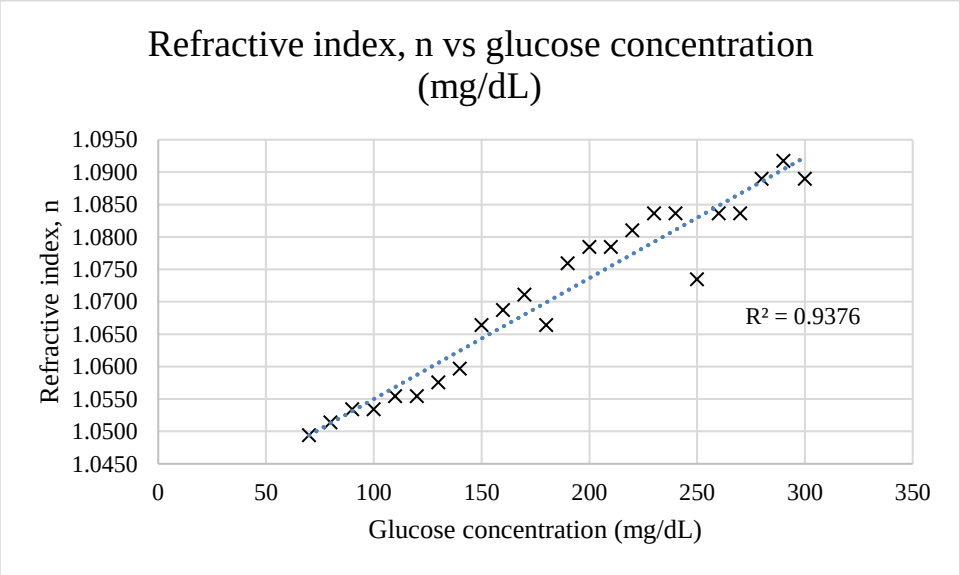

Figure 4.2: Glucose concentration (mg/dL) vs refractive index, n

4.3 Assessing the effects of urine variation on measurement

The prototype was assessed with respect to varying volume, varying turbidity and shelf-life of the urine samples. The assessment of varying volume would determine the effects of varying depth of the sample. Whereas the assessment of varying turbidity would determine the limitation of the prototype in terms of turbidity. As for the assessment of shelf-life study the conditions of the urine samples especially in turbidity up to three days.

4.3.1 Effects of varying volume on measurement

Volumetric assessment was done by varying volumes with the same glucose concentration in order to understand the effects of varying depth of the sample. Based on Table 4.1 varying volumes of samples does not affect the outcome of the results. The change in depth of the sample affect only the planar position of the laser in the beaker as observed in Figure 4.3.

Table 4.1: Results of varying volume and varying glucose levels

Volume (mℓ)	**Concentration of prepared glucose solution**		
	100 (mg/dℓ)	200 (mg/dℓ)	300 (mg/dℓ)
10	804 pixels	740 pixels	678 pixels
20	806 pixels	743 pixels	680 pixels
30	805 pixels	739 pixels	680 pixels
40	803 pixels	738 pixels	677 pixels
50	806 pixels	737 pixels	678 pixels
Average	804.8 pixels	739.4 pixels	678.6 pixels
Std dev	1.303	2.302	1.341

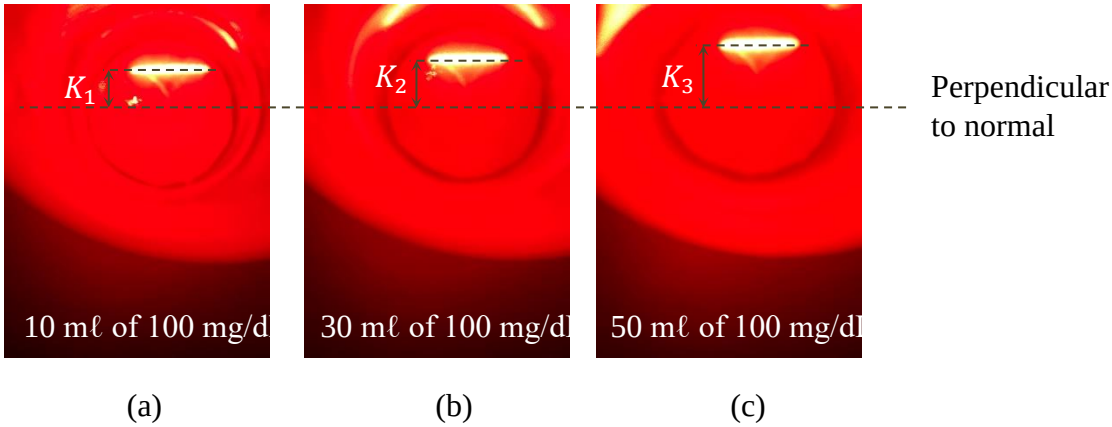

Figure 4.3: Planar position of measured laser line in (a) 10 mℓ of 100 mg/dL, (b) 30 mℓ of 100 mg/dL, and (c) 50 mℓ of 100 mg/dL glucose solutions

Based on Figure 4.4, by using trigonometry, it can be written that

$$\theta_r = tan^{-1}\left(\frac{K_r}{h}\right) \qquad \text{Equation 4.1}$$

Where $K_r$the position of is refracted laser line on the base of the container and h is the liquid depth of the sample from the base of the container.

By rearranging Equations 3.1 ($\frac{n_{air}}{n_{urine}} = \frac{\sin\theta_r}{\sin\theta_i}$) and 4.1, any variation of liquid depth would only affect the planar position of the refracted laser on the base of the container as given in Equation 4.2. In other words, K_r is directly proportional to h.

$$n_{urine} = \frac{\sin\theta_i}{\sin\left[\tan^{-1}\left(\frac{K_r}{h}\right)\right]} \qquad \text{Equation 4.2}$$

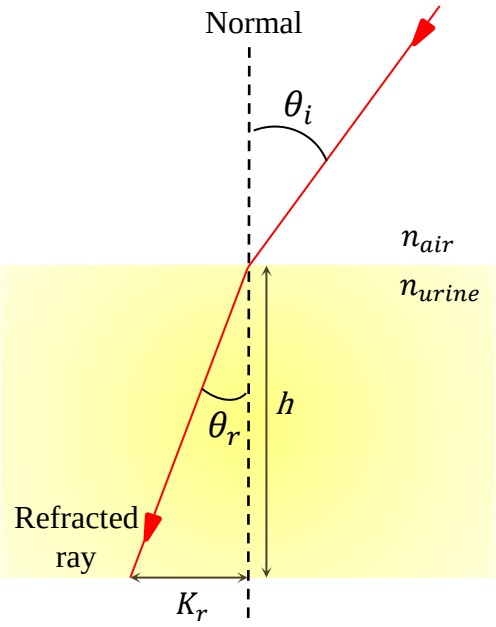

Figure 4.4: Detailed side view of sample with higher glucose concentration

4.3.2 Effects of varying turbidity on measurement

Human urine can come in different turbidity and colour as observed in Figure 4.5. Turbidity in urine can be caused by numerous factors such as bacteria, pus, blood, crystals, protein and more (Simerville et al. (2005)). The next tesout determines how different turbidity would affect the results of the proposed prototype. The samples in this test were done as mentioned in the previous chapter using food grade coffee powder mixed with water.

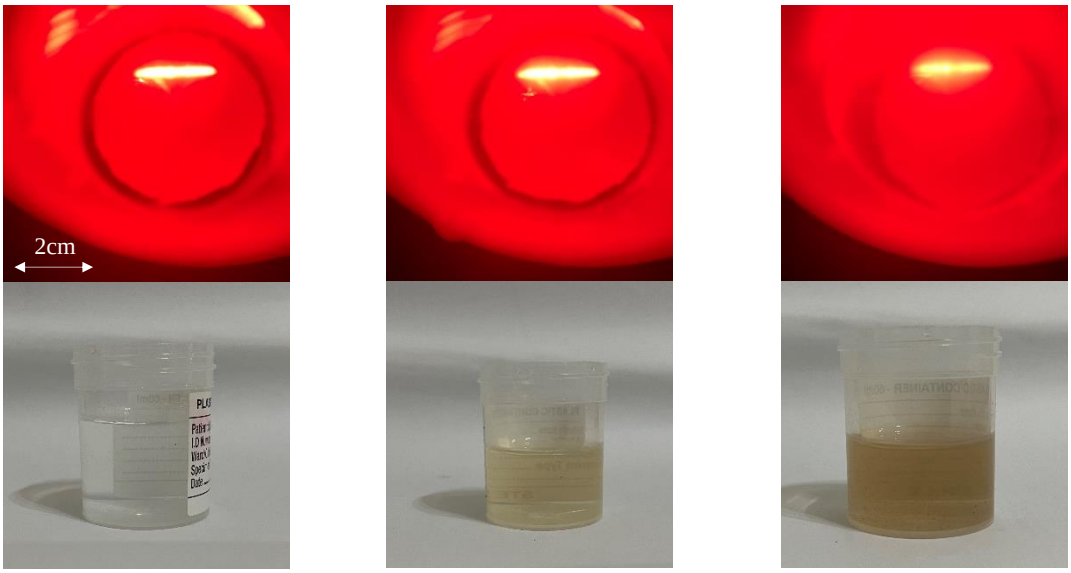

(a) (b) (c)

Figure 4.5: Image of sample with turbidity of (a) 0 NTU, (b) 57 NTU, and (c) 106 NTU

Table 4.2: Results of Nephelometer and corresponding smartphone-based laser refractometer results

Sample	Mass (g)	Nephelometric turbidity unit (NTU)	Image 1 (pixels)	Image 2 (pixels)	Image 3 (pixels)	Average (pixels)
1	0.00	0	825	828	827	826.67
2	0.25	26	821	822	823	822.00
3	0.50	57	816	814	814	814.67
4	0.75	75	-	-	-	-
5	1.00	106	-	-	-	-
6	1.25	131	-	-	-	-
7	1.50	148	-	-	-	-
8	1.75	179	-	-	-	-
9	2.00	190	-	-	-	-
10	2.25	228	-	-	-	-

From Table 4.2 it can be confirmed that there is a limit on how high turbidity can be for the proposed prototype, hence showcasing a weakness. For fabricated and actual samples, the NTU levels of the samples have to be about 57 NTU and under. The average NTU levels of human urine is 30 NTU (Sintawardani et al. (2023). It is also worth mentioning that the NTU levels of urine can be reduced by undergoing the urine samples in a centrifuge. Alternatively, leaving the urine sample to rest for 30 minutes to 1 hour will eventually let the sediments settle down to the bottom of its container hence leaving clear urine on top. This was further proven using MATLAB to determine the intensity of the measured laser lengths as in Figure 4.6. This showed that the intensity profile deteriorated when the sample was at 75 NTU further proving that the limit of the proposed design is 57 NTU.

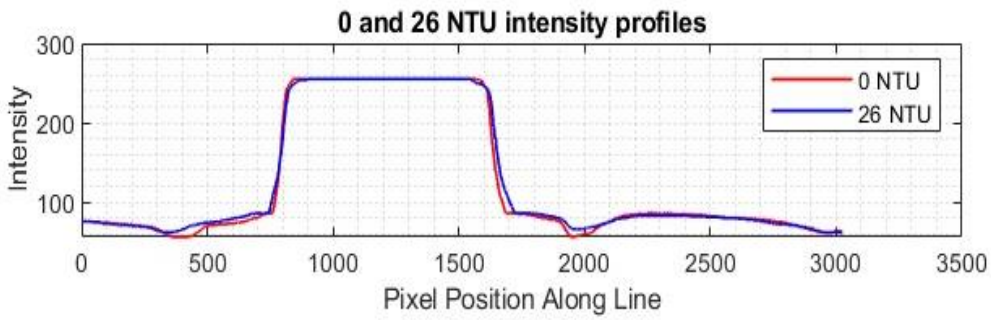

(a)

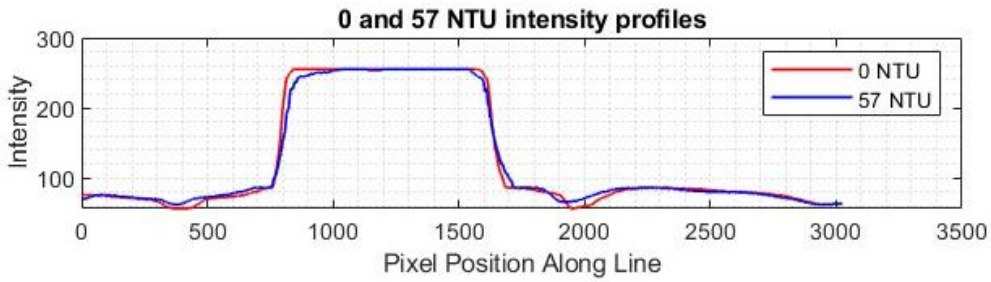

(b)

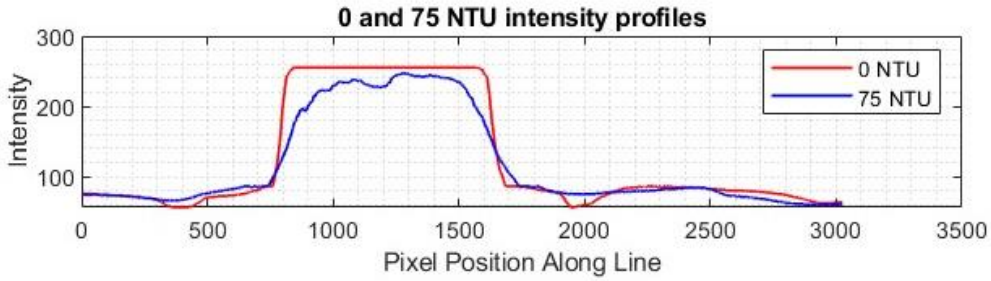

(c)

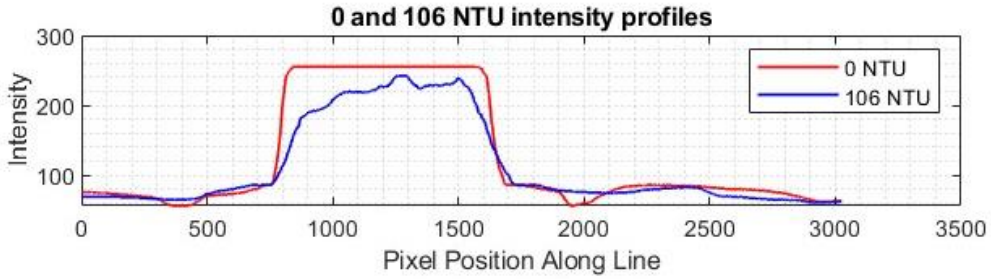

(d)

Figure 4.6: Intensity profile comparisons of 0 NTU with (a) 26 NTU, (b) 57 NTU, (c) 75 NTU, and (d) 106 NTU

4.3.3 Effects of shelf-life on measurement

To ensure that the shelf-life of the samples does not affect the results, this test determine the outcome if the samples were read at different times. Samples are used with the proposed prototype on the day of acquisition, after 1 day and after 2 days. Three images of the samples are taken to obtain the mean reading. The results in Table 4.3 showed that the standard deviation from three days ranged from 0.19 – 6.30 indicating an acceptable level of variability considering the simplicity of the proposed method especially if the proposed method is for routine use rather than clinical use. The samples are refrigerated and kept in airtight screw containers to avoid the occurrence of oxidization. Oxidization of urine can affect its chemical, biological, physiological and physical characteristics through either urea

decomposition, creatinine alteration, protein breakdown or colorimetric changes (Gharsallah et al. (2018). For example, creatinine alteration will change the concentration of the urine samples and thus affect the refractive index (Gharsallah et al. (2018).

Table 4.3: Smartphone-based laser refractometer results after 5 hours, 1 day and 2 days of sample acquired on 2nd and 23rd August 2024

Sample No.	**mg/dL**	**Smartphone-based laser refractometer (pixels)**					**Smartphone-based laser refractometer (mg/dL)**
		After 5 hours	**After 1 day**	**After 2 days**	**Mean**	**Std dev**	
c17	81	867.00	867.33	867.00	867.11	0.19	76.87
c3	84.6	868.33	866.00	868.33	867.56	1.35	70.47
c9	84.6	863.33	865.33	865.33	864.67	1.15	94.47
c1	86.4	862.67	863.33	865.00	863.67	1.20	97.67
c4	86.4	862.67	863.33	862.67	862.89	0.38	97.67
b11	100.8	867.00	866.33	867.67	867.00	0.67	76.87
b5	113.4	865.00	866.67	865.67	865.78	0.84	86.47
c10	117	860.67	860.67	861.00	860.78	0.19	107.27
c12	118.8	860.00	860.33	860.33	860.22	0.19	110.47
b1	120.6	845.00	842.67	847.67	845.11	2.50	182.47
b9	122.4	851.33	850.67	851.67	851.22	0.51	152.07
b4	126	848.33	849.33	848.00	848.56	0.69	166.47
b2	133.2	848.33	849.33	848.00	848.56	0.69	166.47
c18	135	850.33	850.33	845.00	848.56	3.08	156.87

Table 4.3: Continued

c5	142.2	843.33	842.00	847.67	844.33	2.96	190.47
c21	142.2	842.00	841.67	843.00	842.22	0.69	196.87
c7	156.6	842.33	839.67	843.67	841.89	2.04	195.27
b7	176.4	846.67	847.67	845.67	846.67	1.00	174.47
c16	180	850.67	838.67	841.33	843.56	6.30	155.27
c19	180	837.33	836.00	839.33	837.56	1.68	219.27
b10	205.2	838.67	839.67	840.00	839.44	0.69	212.87
b16	234	833.33	832.67	835.00	833.67	1.20	238.47
b14	279	833.00	833.67	830.67	832.44	1.58	240.07
c14	286.2	831.67	831.67	832.67	832.00	0.58	246.47
c8	349.2	824.67	825.67	827.00	825.78	1.17	280.07
b8	487.8	818.33	819.00	818.67	818.67	0.33	310.46

4.4 Actual urine

Once the smartphone-based laser refractometer was tested and calibrated, then the actual urine was tested. Urine samples collected are provided with blood analysis and urinalysis results. Results of the actual urine using the smartphone-based laser refractometer are compared with the fasting glucose levels from the blood report but not the urinalysis results. This is because urinalysis results are in a range instead of an integer value which makes it difficult for comparison.

4.4.1 Comparison with fasting glucose levels

The first comparison is with a total of 93 fasting glucose levels from the APSB and PBP. Only 93 of the 160 samples were viable for the proposed method because the remaining 67 were cloudy therefore not viable with the proposed method. The raw data shows promising results of the proposed method having the highest standard deviation of 5.86. By referring to Figure 4.7, the results from this comparison had a correlation coefficient, R^2 = 0.8881 with a sensitivity of 4.8 mg/dL.

It is important to note that bilirubin (byproduct of hemoglobin), ketones (byproduct of fat) and proteinuria (protein) are present in liquid form in urine samples Çelik et al. (2024); Pape et al. (2020), and Ridley (2018). These substances can influence the refractive index of urine, potentially affecting measurement accuracy Bökenkamp (2020); Kumar et al. (2018), and Portincasa et al. (2023). In some cases, bilirubin may exist in the form of crystals which may affect turbidity. In this study, 11 samples reported proteinuria, three reported ketones and none reported bilirubin presence. Of the 11 samples that reported proteinuria presence, only two samples were cloudy (sample no. 4558 and 4671). Of the three samples that reported ketones presence, two samples were cloudy (sample no. 4628 and 4840f). Due to the relatively high turbidity, these four samples were unusable and therefore omitted. Of the many samples collected, there was one sample (sample no. 4844) being omitted as well due to the considerably high presence of protein and ketone.

From the total of 160 samples collected, 67 samples were found to be slightly cloudy or cloudy since the NTU level is approximately more than the detectability of proposed prototype. Cloudy urine may be caused by the presence of pus, bacteria, blood, crystals, protein and more (Simerville et al. (2005)). However, 18 samples were slightly cloudy (less

than 57 NTU) and were still viable to be used with the proposed refractometer as proven in turbidity assessment section. This proved a weakness because samples must be clear/slightly cloudy with the absence of bilirubin, protein and/or ketones for the best results. This can be addressed using advanced digital image processing algorithms which will be the subject of our future study.

Figure 4.7 shows the results of the smartphone-based laser refractometer and fasting glucose concentration obtained from the samples. The graph shows a correlation coefficient of 0.89 suggesting the potential of the proposed device as a viable alternative for glucose monitoring. It can also be observed that outliers are present in the results. However, it can be alleged that because these samples are from PBP which uses a conventional glucometer, the levels of ketones, proteins and bilirubin are unattainable which could affect the results as discussed above.

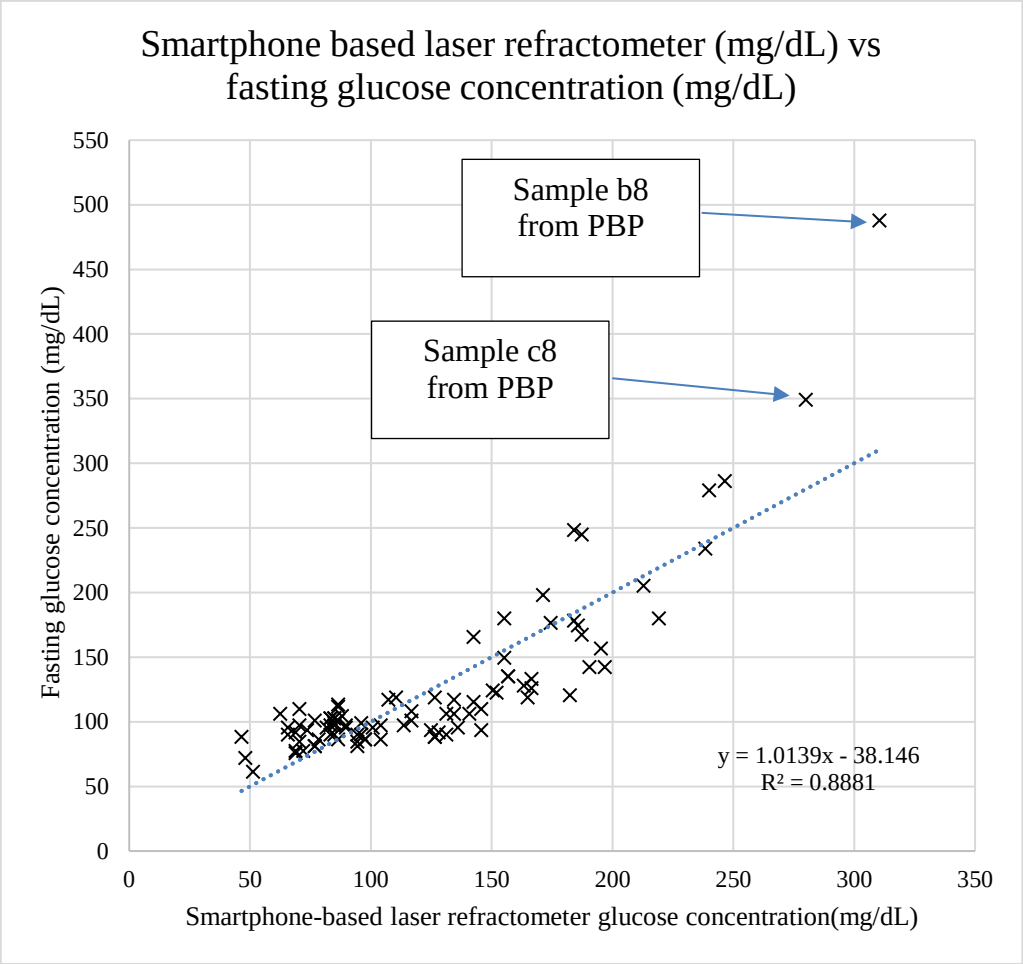

Figure 4.7: Smartphone-based laser refractometer (mg/dL) vs fasting glucose concentrations (mg/dL)

Table 4.4 compares the smartphone-based laser refractometer with previous research on colorimetry based on limit of detection and correlation coefficient. For colorimetry of test strips in Pohanka et al. (2024), R^2 of 0.998 and sensitivity of 1.98 mg/dL was obtained. While works in colorimetry of AuNPs such as Feng et al. (2023) and Firdaus et al. (2022) resulted in R^2 of 0.876 and 0.998 and sensitivity of 0.0002 and 0.00008 mg/dL, respectively. Although the present method demonstrates a higher limit of detection and a lower correlation coefficient compared to other proposed methods, it offers notable advantages in terms of simplicity, cost-effectiveness, and user-friendliness. In contrast to other urinalysis methods

that often require expensive instrumentation and complex procedures, the proposed approach utilizes a more accessible and straightforward setup. As a result, it holds greater potential for real-world implementation, particularly in resource-limited settings or for point-of-care applications.

Table 4.4: Comparison of previous urinalysis methods for glucose sensing

Method of urinalysis	**Limit of detection (mg/dL)**	**Correlation Coefficient, R^2**	**Ref.**
Colorimetry of test strips	1.98	0.998	Pohanka et al. (2024)
Colorimetry of AuNPs	0.0002	NA	Feng et al. (2023)
Colorimetry of AuNPs	0.00008	0.99	Firdaus et al. (2022)
Biosensors (GOx)	0.103	0.99	Hajimiri et al. (2023)
Biosensors (ZnS)	2.3	NA	Nguyen et al. (2023)
Biosensors (GOx)	0.0007	0.95	Fenoy et al. (2022)
Smartphone-based laser refractometer	4.8	0.89	Present work

4.5 Sensitivity, specificity, positive predictive values and negative predictive values

Based on Table 4.5, the proposed prototype has a sensitivity of 1 and NPV of 0. Whereas the specificity and PPV are 0.61 and 0.76 respectively. This means that the prototype performs well to determine when a patient has the disease with zero false negative results. However, false positive results are relatively high showing weakness of the prototype for negative patients. More samples can be acquired to further improve or investigate the

specificity and PPV of the proposed prototype. By acquiring more samples, the impact of random variation is minimized, leading to more accurate and reliable estimates of the research's performance. The increase in precision enhances the likelihood of correctly identifying true positive and true negative cases, thereby strengthening the validity of the sensitivity, specificity, PPV and NPV.

Table 4.5: True positive (TP), true negative (TN), false positive (FP) and false negative (FN) results from smartphone-based laser refractometer

Prototype Results	**Disease**	
	Has disease	**No disease**
+	TP (52)	FP (16)
-	FN (0)	TN (25)

CHAPTER 5

CONCLUSION AND RECOMMENDATIONS

5.1 Conclusion

The following conclusions can be derived from this study;

i. A non-contact smartphone-based laser refractometer for glucose monitoring was successfully developed. The refractive indices of the urine, based on the refracted length of the laser line, were correlated with fasting blood glucose concentrations. The proposed prototype uses a smartphone to capture a relatively high resolution images of a laser line caused by total internal reflection through the rod and refraction caused by the urine (Objective 1).

ii. With the developed prototype, assessment was done in three parts: volumetric, turbidity and shelf-life assessments. For volumetric, assessment was done with a constant glucose concentration but varying volume levels. The results from this section gave a consistent pixel count for each concentration which proved that volume is not a crucial factor in measuring glucose levels using the smartphone-based laser refractometer. This is because the volume of the samples would only affect the planar position of the laser line in the images. As for turbidity, the assessment was done with prepared samples with varying levels of turbidity (NTU). For this assessment, it was done to test the limits of the smartphone-based laser refractometer in terms of turbidity which was found to be 57 NTU which is higher than the average turbidity of human urine as reported in the literature. Assessment based on shelf-life was also done where the samples were still viable after three days

of collection. It is reported that there is little to no change in the readings with a standard deviation ranging from 0.19 to 6.30 (Objective 2).

iii. Once assessed, the smartphone-based laser refractometer was used with actual urine samples. For this, urine samples were collected from APSB and PBP on a weekly basis for assessment using the proposed prototype. Urine samples collected come with a blood report (fasting) and urinalysis report for comparison of results using the prototype. For fasting (blood report) glucose levels, the achieved correlation coefficient, $R^2 = 0.89$ with a limit of detection of 4.8 mg/dL (Objective 3).

5.2 Recommendations

i. The application of neural networks and machine learning algorithms to precisely determine the length of the refracted laser line in the presence of high turbidity in urine samples will overcome the limitations of the current study, which relies on manual interpretation.

ii. Development and integration of smartphone applications to further improve usability, especially for telemedicine purposes.

REFERENCES

Abbott. (2018). Freestyle LibreTM. [online] Availabe at: https://www.freestylelibre.us/ [Assessed on 3 Februrary 2019]

Alam, M. M., Saha, S., Saha, P., Nur, F. N., Moon, N. N., Karim, A., & Azam, S. (2020). D-care: A non-invasive glucose measuring technique for monitoring diabetes patients. In *Proceedings of International Joint Conference on Computational Intelligence: IJCCI 2018*, 443-453. Springer Singapore..

Bezuglyi, M., Bezuglaya, N., Kuprii, O., & Yakovenko, I. (2018). The non-invasive optical glucometer prototype with ellipsoidal reflectors. In *Proceedings of 59th International Scientific Conference on Power and Electrical Engineering of Riga Technical University (RTUCON)*, 1-4. IEEE.

Bökenkamp, A. (2020). Proteinuria—take a closer look! *Pediatric Nephrology*, *35*(4), 533-541.

Bollella, P., Sharma, S., Cass, A. E. G., Tasca, F., & Antiochia, R. (2019). Minimally Invasive Glucose Monitoring Using a Highly Porous Gold Microneedles-Based Biosensor: Characterization and Application in Artificial Interstitial Fluid. *Catalysts*, *9*(7), 210-219.

Cebedio, M. C., Rabioglio, L. A., Gelosi, I. E., Ribas, R. A., Uriz, A. J., & Moreira, J. C. (2020). Analysis and Design of a Microwave Coplanar Sensor for Non-Invasive Blood Glucose Measurements. *IEEE Sensors Journal*, *20*(18), 10572-10581.

Çelik, H., Caf, B. B., Geyik, C., Çebi, G., & Tayfun, M. (2024). Enhancing urinalysis with smartphone and AI: a comprehensive review of point-of-care urinalysis and nutritional advice. *Chemical Papers*, *78*(2), 651-664.

Chen, H., & Li, R. (2021). Introduction of Diabetes Mellitus and Future Prospects of Natural Products on Diabetes Mellitus. In H. Chen & M. Zhang (Eds.), *Structure and Health Effects of Natural Products on Diabetes Mellitus* (pp. 1-15). Singapore: Springer Singapore.

Chinnadayyala, S. R., park, J., Satti, A. T., Kim, D., & Cho, S. (2021). Minimally invasive and continuous glucose monitoring sensor based on non-enzymatic porous platinum black-coated gold microneedles. *Electrochimica Acta*, *369*, 137691.

Dexcom. (2018a). Platinum G6®. [online] Availabe at: https://www.dexcom.com/g5-mobile-cgm [Assessed on 3 Februrary 2019]

Dexcom. (2018b). Platinum G5®. [online] Availabe at: from https://www.dexcom.com/g6- cgm-system [Assessed on 3 Februrary 2019]

Diez Alvarez, S., Fellas, A., Santos, D., Sculley, D., Wynne, K., Acharya, S., . . . Coda, A. (2023). The Clinical Impact of Flash Glucose Monitoring—a Digital Health App and Smartwatch Technology in Patients With Type 2 Diabetes: Scoping Review. *JMIR Diabetes*, *8*, e42389.

Dutta, A., Chandra Bera, S., & Das, K. (2019). A non-invasive microcontroller based estimation of blood glucose concentration by using a modified capacitive sensor at low frequency. *AIP Advances*, *9*(10), 105027.

Egan, A. M., & Dinneen, S. F. (2019). What is diabetes? *Medicine*, *47*(1), 1-4.

Feng, F., Ou, Z., Zhang, F., Chen, J., Huang, J., Wang, J., Zeng, J. (2023). Artificial intelligence-assisted colorimetry for urine glucose detection towards enhanced sensitivity, accuracy, resolution, and anti-illuminating capability. *Nano Research, 16*(10), 12084-12091.

Fenoy, G. E., Marmisollé, W. A., Knoll, W., & Azzaroni, O. (2022). Highly sensitive urine glucose detection with graphene field-effect transistors functionalized with electropolymerized nanofilms. *Sensors & Diagnostics, 1*(1), 139-148.

Firdaus, M. L., Saputra, E., Ginting, S. M., Wyantuti, S., Eddy, D. R., Rahmidar, L., & Yuliarto, B. (2022). Smartphone-based digital image colorimetry for non-enzymatic detection of glucose using gold nanoparticles. *Sensing and Bio-Sensing Research, 35*, 100472.

Galicia-Garcia, U., Benito-Vicente, A., Jebari, S., Larrea-Sebal, A., Siddiqi, H., Uribe, K. B., Martín, C. (2020). Pathophysiology of Type 2 Diabetes Mellitus. *International Journal of Molecular Sciences, 21*(17), 6275.

Gharsallah, Z., Najjar, M., Suthar, B., & Janyani, V. (2018). High sensitivity and ultra-compact optical biosensor for detection of UREA concentration. *Optical and Quantum Electronics, 50*(6), 249-261.

Gonzales, V. W., Mobashsher, A. T., & Abbosh, A. (2019). The Progress of Glucose Monitoring: A Review of Invasive to Minimally and Non-Invasive Techniques, Devices and Sensors. *Sensors, 19*(4), 301-312.

Hajimiri, H., Safiabadi Tali, S. H., Al-Kassawneh, M., Sadiq, Z., & Jahanshahi-Anbuhi, S. (2023). Tablet-Based Sensor: A Stable and User-Friendly Tool for Point-of-Care Detection of Glucose in Urine. *Biosensors, 13*(9), 101-109.

Hanna, J., Bteich, M., Tawk, Y., Ramadan, A. H., Dia, B., Asadallah, F. A., Eid, A. A. (2020). Noninvasive, wearable, and tunable electromagnetic multisensing system for continuous glucose monitoring, mimicking vasculature anatomy. *Science Advances, 6*(24), 5320.

Hanna, J., Tawk, Y., Azar, S., Ramadan, A. H., Dia, B., Shamieh, E., Eid, A. A. (2022). Wearable flexible body matched electromagnetic sensors for personalized non-invasive glucose monitoring. *Scientific Reports, 12*(1), 14885.

Jain, P., Maddila, R., & Joshi, A. M. (2019). A precise non-invasive blood glucose measurement system using NIR spectroscopy and Huber's regression model. *Optical and Quantum Electronics, 51*(2), 51-62.

Jiang, S., Zhang, Y., Yang, Y., Huang, Y., Ma, G., Luo, Y., Lin, J. (2019). Glucose Oxidase-Instructed Fluorescence Amplification Strategy for Intracellular Glucose Detection. *ACS Applied Materials & Interfaces, 11*(11), 10554-10558.

Karpova, E. V., Shcherbacheva, E. V., Galushin, A. A., Vokhmyanina, D. V., Karyakina, E. E., & Karyakin, A. A. (2019). Noninvasive Diabetes Monitoring through Continuous Analysis of Sweat Using Flow-Through Glucose Biosensor. *Analytical Chemistry, 91*(6), 3778-3783.

Kasahara, R., Kino, S., Soyama, S., & Matsuura, Y. (2018). Noninvasive glucose monitoring using mid-infrared absorption spectroscopy based on a few wavenumbers. *Biomedical Optics Express, 9*(1), 289-302.

Kaul, K., Tarr, J. M., Ahmad, S. I., Kohner, E. M., & Chibber, R. (2013). Introduction to Diabetes Mellitus. In S. I. Ahmad (Ed.), *Diabetes: An Old Disease, a New Insight* (pp. 1-11). New York, NY: Springer New York.

Kavitha, S., & Murthy, V. R. (2006). Refractometry as a tool in diabetic studies. *Anc Sci Life, 25*(3-4), 76-83.

Kumar, V., & Gill, K. D. (2018). Qualitative Analysis of Ketone Bodies in Urine. In V. Kumar & K. D. Gill (Eds.), *Basic Concepts in Clinical Biochemistry: A Practical Guide* (pp. 119-122). Singapore: Springer Singapore.

Li, N., Zang, H., Sun, H., Jiao, X., Wang, K., Liu, T. C., & Meng, Y. (2019). A Noninvasive Accurate Measurement of Blood Glucose Levels with Raman Spectroscopy of Blood in Microvessels. *Molecules, 24*(8), 1500-1511.

Lin, P.-H., Sheu, S.-C., Chen, C.-W., Huang, S.-C., & Li, B.-R. (2022). Wearable hydrogel patch with noninvasive, electrochemical glucose sensor for natural sweat detection. *Talanta, 241*, 123187.

Lipani, L., Dupont, B. G. R., Doungmene, F., Marken, F., Tyrrell, R. M., Guy, R. H., & Ilie, A. (2018). Non-invasive, transdermal, path-selective and specific glucose monitoring via a graphene-based platform. *Nature Nanotechnology, 13*(6), 504-511.

Lockwood (Eds.), *Urine Tests: A Case-Based Guide to Clinical Evaluation and Application* (pp. 117-141). Cham: Springer International Publishing.

Lovic, D., Piperidou, A., Zografou, I., Grassos, H., Pittaras, A., & Manolis, A. (2020). The Growing Epidemic of Diabetes Mellitus. *Current Vascular Pharmacology, 18*(2), 104-109.

Lu, Q., Huang, T., Zhou, J., Zeng, Y., Wu, C., Liu, M., Yao, S. (2021). Limitation-induced fluorescence enhancement of carbon nanoparticles and their application for glucose detection. *Spectrochimica Acta Part A: Molecular and Biomolecular Spectroscopy, 244*, 118893.

Lundsgaard-Nielsen, S. M., Pors, A., Banke, S. O., Henriksen, J. E., Hepp, D. K., & Weber, A. (2018). Critical-depth Raman spectroscopy enables home-use non-invasive glucose monitoring. *PLOS ONE, 13*(5), e0197134.

Monaghan, T. F., Rahman, S. N., Agudelo, C. W., Wein, A. J., Lazar, J. M., Everaert, K., & Dmochowski, R. R. (2021). Foundational Statistical Principles in Medical Research: Sensitivity, Specificity, Positive Predictive Value, and Negative Predictive Value. *Medicina, 57*(5), 319-332.

Nemaura. (2018). SugarBEAT®. [online] Availabe at: http://sugarbeat.com/ [Assessed on 3 Februrary 2019]

Nguyen, S. H., Vu, P. K., Nguyen, H. M., & Tran, M. T. (2023). Optical Glucose Sensors Based on Chitosan-Capped ZnS-Doped Mn Nanomaterials. *Sensors, 23*(5), 5121-5135.

Nie, F., Ga, L., Ai, J., & Wang, Y. (2020). Trimetallic PdCuAu Nanoparticles for Temperature Sensing and Fluorescence Detection of H2O2 and Glucose. *Frontiers in Chemistry, 8*(2), 244-259.

Omer, A. E., Shaker, G., Safavi-Naeini, S., Kokabi, H., Alquié, G., Deshours, F., & Shubair, R. M. (2020). Low-cost portable microwave sensor for non-invasive monitoring of blood glucose level: novel design utilizing a four-cell CSRR hexagonal configuration. *Scientific Reports*, *10*(1), 15200-15213.

Pape, P. T., Sharp, V. J. A., & Rockafellow, J. (2020). Urine Dipstick: An Approach to Glucosuria, Ketonuria, pH, Specific Gravity, Bilirubin and Urobilinogen – Undeniable Chemistry. In V. J. A. Sharp, L. M. Antes, M. L. Sanders, & G. M. Lockwood (Eds.), *Urine Tests: A Case-Based Guide to Clinical Evaluation and Application* (pp. 117-141). Cham: Springer International Publishing.

Pighi, L., Negrini, D., Henry, B. M., Salvagno, G. L., & Lippi, G. (2023). Urine dipstick for screening plasma glucose and bilirubin in low resource settings: a proof-of-concept study. *Advances in Laboratory Medicine/Avances en Medicina de Laboratorio*, *4*(4), 431-434.

Pohanka, M., & Zakova, J. (2024). Urine Test Strip Quantitative Assay with a Smartphone Camera. *International Journal of Analytical Chemistry*, *1*(1), 6004970.

Portincasa, P., Di Ciaula, A., Bonfrate, L., Stella, A., Garruti, G., & Lamont, J. T. (2023). Metabolic dysfunction-associated gallstone disease: expecting more from critical care manifestations. *Internal and Emergency Medicine*, *18*(7), 1897-1918.

Rachim, V. P., & Chung, W.-Y. (2019). Wearable-band type visible-near infrared optical biosensor for non-invasive blood glucose monitoring. *Sensors and Actuators B: Chemical*, *286*, 173-180.

Rassel, S., Kaysir, M. R., Aloraynan, A., & Ban, D. (2023). Non-invasive blood sugar detection by cost-effective capacitance spectroscopy. *Journal of Sensors and Sensor Systems*, *12*(1), 21-36.

Ribet, F., Stemme, G., & Roxhed, N. (2018). Real-time intradermal continuous glucose monitoring using a minimally invasive microneedle-based system. *Biomedical Microdevices*, *20*(4), 101-113.

Ridley, J. W. (2018). Elements Involved in the Physical Evaluation of Urine. In J. W. Ridley (Ed.), *Fundamentals of the Study of Urine and Body Fluids* (pp. 143-175). Cham: Springer International Publishing.

Sadiq, I. Z., Usman, A., Muhammad, A., & Ahmad, K. H. (2024). Sample size calculation in biomedical, clinical and biological sciences research. *Journal of Umm Al-Qura University for Applied Sciences*, *23*(2), 1-9.

Saleh, G., Alkaabi, F., Al-Hajhouj, N., Al-Towailib, F., & Al-Hamza, S. (2018). Design of non-invasive glucose meter using near-infrared technique. *Journal of Medical Engineering & Technology*, *42*(2), 140-147.

Sempionatto, J. R., Brazaca, L. C., García-Carmona, L., Bolat, G., Campbell, A. S., Martin, A., Wang, J. (2019). Eyeglasses-based tear biosensing system: Non-invasive detection of alcohol, vitamins and glucose. *Biosensors and Bioelectronics*, *137*, 161-170.

Sempionatto, J. R., Moon, J.-M., & Wang, J. (2021). Touch-Based Fingertip Blood-Free Reliable Glucose Monitoring: Personalized Data Processing for Predicting Blood Glucose Concentrations. *ACS Sensors*, *6*(5), 1875-1883.

Senseonics. (2018). EversenseTM. [online] Availabe at: https://www.eversensediabetes.com/ [Assessed on 3 Februrary 2019]

Sim, J. Y., Ahn, C.-G., Jeong, E.-J., & Kim, B. K. (2018). In vivo Microscopic Photoacoustic Spectroscopy for Non-Invasive Glucose Monitoring Invulnerable to Skin Secretion Products. *Scientific Reports, 8*(1), 1059-1071.

Sintawardani, N., Adhilaksma, C. A., Hamidah, U., Pradanawati, S. A., & Suharno, S. M. (2023). Evaluation of human urine purification using rice husk charcoal as the adsorbent. *IOP Conference Series: Earth and Environmental Science, 1201*(1), 012107.

Skrajnowska, D., & Bobrowska-Korczak, B. (2024). The Effects of Diet, Dietary Supplements, Drugs and Exercise on Physical, Diagnostic Values of Urine Characteristics. *Nutrients, 16*(18). Retrieved from doi:10.3390/nu16183141

Sweeting, A., Wong, J., Murphy, H. R., & Ross, G. P. (2022). A Clinical Update on Gestational Diabetes Mellitus. *Endocrine Reviews, 43*(5), 763-793.

Tamrin, K., Adilah, A., Hamdi, M., & Jong, R. (2018). Smartphone-based laser glucometer for non-invasive measurement of glucose level of diabetic patients. *Borneo International Journal, 1*(1), 27-32.

Tanaka, Y., Tajima, T., Seyama, M., & Waki, K. (2020). Differential Continuous Wave Photoacoustic Spectroscopy for Non-Invasive Glucose Monitoring. *IEEE Sensors Journal, 20*(8), 4453-4458.

Tohl, D., Tran Tam Pham, A., Li, J., & Tang, Y. (2024). Point-of-care image-based quantitative urinalysis with commercial reagent strips: Design and clinical evaluation. *Methods, 224*, 63-70.

Yao, Y., Chen, J., Guo, Y., Lv, T., Chen, Z., Li, N., Chen, T. (2021). Integration of interstitial fluid extraction and glucose detection in one device for wearable non-invasive blood glucose sensors. *Biosensors and Bioelectronics, 179*, 113-128.

Zou, Y., Huang, M., Wang, K., Song, B., Wang, Y., Chen, J., Huang, G. (2016). Urine surface-enhanced Raman spectroscopy for non-invasive diabetic detection based on a portable Raman spectrometer. *Laser Physics Letters, 13*(6), 60-69.

APPENDICES

Appendix A – Experimental results of preliminary tests using prepared glucose samples

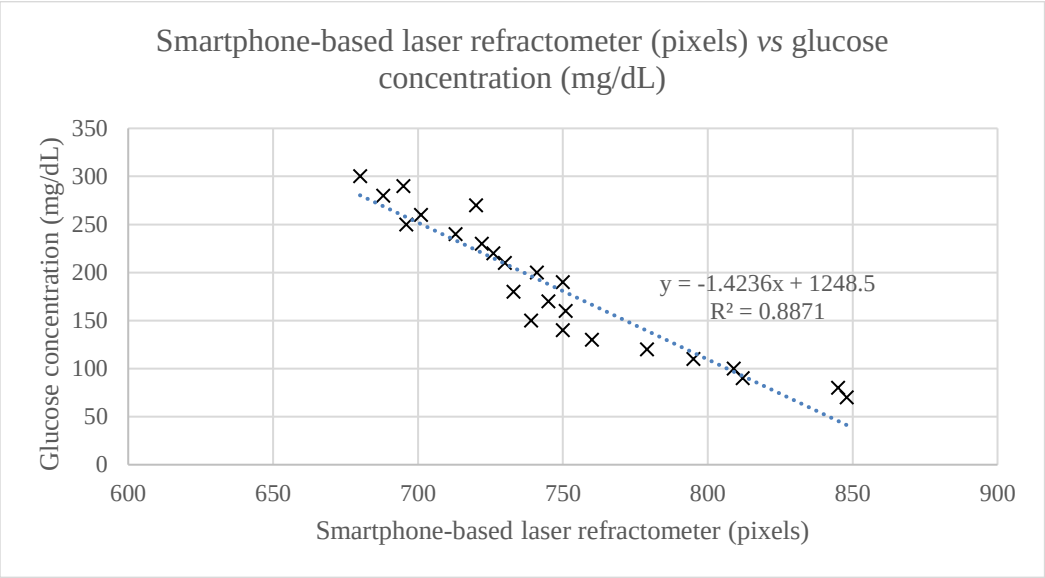

Figure A: Smartphone-based laser refractometer (pixels) *vs* glucose concentration (mg/dL)

Table A: Results of preliminary tests using prepared glucose samples

Glucose concentration (mg/dL)	Pixel count	Smartphone-based laser refractometer (mg/dL)
70	848	50.816
80	845	51.987
90	812	72.596
100	809	75.171
110	795	88.737
120	779	107.361
130	760	133.800
140	750	149.600

150	739	168.481
160	751	147.961
170	745	157.987
180	733	179.443
190	750	149.600
200	741	164.931
210	730	185.100
220	726	192.824
230	722	200.756
240	713	219.363
250	696	257.384
260	701	245.811
270	720	204.800
280	688	276.576
290	695	259.737
300	680	296.600

From the equation in Figure A, the equation is used to determine the mg/dL value using the pixels obtained. In this case, $x = (0.0065)(pixels^2) - (11.395)(pixels) + 5039.6$

Appendix B – Experimental results of actual urine compared with fasting glucose levels

Table B: Results of fasting glucose levels (mg/dL) from APSB and PBP with the corresponding measurements using smartphone-based laser refractometer (pixels)

From	Sample no.	Fasting (mg/dL)	pH	Turbidity	Debris	Protein	Ketones	Bilirubin	Image 1	Image 2	Image 3	Average	Std dev.
APSB	4440	99	6.5	clear	no	neg	neg	neg	860	866	863	863.00	3.00
APSB	4442	93.6	5	clear	no	neg	neg	neg	867	867	869	867.67	1.15
APSB	4443	108	6	clear	no	neg	neg	neg	860	856	860	858.67	2.31
APSB	4446	374.4	5	clear	no	neg	neg	neg	850	848	847	848.33	1.53
APSB	4460	100.8	7	clear	no	neg	neg	neg	868	864	863	865.00	2.65
APSB	4463	72	7	clear	no	neg	neg	neg	872	871	876	873.00	2.65
APSB	4467	118.8	5	clear	no	neg	neg	neg	858	853	859	856.67	3.21
APSB	4468		5	slight	slight	neg	neg	neg	853	853	856	854.00	1.73
APSB	4469	95.4	7.5	clear	no	neg	neg	neg	856	857	851	854.67	3.21
APSB	4470	86.4	7.5	clear	no	neg	neg	neg	870	865	865	866.67	2.89
APSB	4471	84.6	8	clear	no	neg	neg	neg	851	849	851	850.33	1.15
APSB	4474		6.5	clear	no	neg	neg	neg	845	850	848	847.67	2.52
APSB	4475		6	clear	no	neg	neg	neg	863	864	857	861.33	3.79
APSB	4476		7	cloudy	yes	neg	neg	neg	-	-	-	-	-
APSB	4477		5	slightly cloudy	slight	neg	neg	neg	856	865	859	860.00	4.58
APSB	4478		6	very cloudy	yes	neg	neg	neg	-	-	-		
APSB	4479		8.5	cloudy	yes	neg	neg	neg	858	854	859	857.00	2.65
APSB	4480		5	slightly cloudy	slight	neg	neg	neg	855	850	851	852.00	2.65
APSB	4481		5	very cloudy	yes	neg	neg	neg	-	-	-		-
APSB	4482		6	clear	no	neg	neg	neg	831	824	822	825.67	4.73
APSB	4509		5.5	clear	no	neg	neg	neg	838	834	834	835.33	2.31
APSB	4513		7.5	clear	no	neg	neg	neg	851	856	853	853.33	2.52
APSB	4514		6	very cloudy	yes	neg	neg	neg	-	-	-		
APSB	4515		6	very cloudy	very	neg	neg	neg	-	-	-		
APSB	4516		6.5	clear	no	neg	neg	neg	845	838	842	841.67	3.51
APSB	4523		6	cloudy	bubbles	neg	neg	neg	763	745	748	752.00	9.64
APSB	4531		6.5	clear	bubbles	neg	neg	neg	839	840	840	839.67	0.58
APSB	4544		5	clear	bubbles	neg	neg	neg	838	836	836	836.67	1.15
APSB	4584	75.6	5	clear	no	neg	neg	neg	873	871	862	868.67	5.86
APSB	4561	79.2	7.5	slightly cloudy	no	neg	neg	neg	833	835	838	835.33	2.52
APSB	4572	81	6.5	clear	no	neg	neg	neg	867	864	870	867.00	3.00
APSB	4574	81	7	clear	no	neg	neg	neg	869	862	859	863.33	5.13
APSB	4580	84.6	5.5	slightly cloudy	no	neg	neg	neg					
APSB	4556	88.2	7.5	clear	no	neg	neg	neg	857	856	857	856.67	0.58
APSB	4559	88.2	6.5	slightly cloudy	no	neg	neg	neg					
APSB	4583	90	7	clear	no	neg	neg	neg	858	853	856	855.67	2.52
APSB	4564	93.6	7.5	clear	no	neg	neg	neg	856	850	852	852.67	3.06

APSB	4560	99	5	slightly cloudy	no	neg	neg	neg					
APSB	4581	100.8	6	clear	no	neg	neg	neg	863	855	858	858.67	4.04
APSB	4570	108	7	clear	no	neg	neg	neg	835	826	822	827.67	6.66
APSB	4571	108	6	very cloudy	yes	neg	neg	neg					
APSB	4558	111.6	7.5	murky	no	1+0.3 g/L	neg	neg					
APSB	4610	81	5.5	Cloudy	slight	neg	neg	neg	-	-	-	-	-
APSB	4611	84.6	7	Clear	no	neg	neg	neg	864	868	865	865.67	2.08
APSB	4608	88.2	7.5	Clear	no	neg	neg	neg	877	871	871	873.00	3.46
APSB	4627	90	7	clear	no	neg	neg	neg	861	864	866	863.67	2.52
APSB	4639	93.6	7.5	Clear	no	neg	neg	neg	851	853	849	851.00	2.00
APSB	4606	95.4	6.5	Clear	no	neg	neg	neg	866	868	862	865.33	3.06
APSB	4612	97.2	8.5	Slightly cloudy	no	neg	neg	neg	-	-	-	-	-
APSB	4628	100.8	9	Slightly cloudy	no	1+0.3 g/L	neg	neg	854	861	857	857.33	3.51
APSB	4605		7.5	Slightly cloudy	no	neg	neg	neg	867	872	869	869.33	2.52
APSB	4635	100.8	6	Cloudy	yes	neg	neg	neg	-	-	-	-	-
APSB	4630	104.4	5.5	Slightly cloudy	yes	neg	neg	neg	849	855	852	852.00	3.00
APSB	4609	106.2	6	Clear	no	2+1.0 g/L	neg	neg	870	873	872	871.67	1.53
APSB	4640	115.2	6	Clear	no	neg	neg	neg	867	866	860	864.33	3.79
APSB	4644	115.2	7	Clear	no	neg	neg	neg	867	865	866	866.00	1.00
APSB	4623		6	Clear	yes	neg	neg	neg	867	864	866	865.67	1.53
APSB	4625		7	clear	yes	neg	neg	neg	-	-	-	-	-
APSB	4637			Cloudy	yes	neg	neg	neg	-	-	-	-	-
APSB	4604		7.5	Slightly cloudy	no	neg	neg	neg	865	864	866	865.00	1.00
APSB	4634	189	5	Clear	no	neg	neg	neg	848	850	853	850.33	2.52
APSB	4656	86.4	7.5	clear	no	neg	neg	neg	861	860	863	861.33	1.53
APSB	4661	88.2	7.5	clear	no	neg	neg	neg	858	858	854	856.67	2.31
APSB	4658	91.8	7	slightly cloudy	no	neg	neg	neg	837	835	839	837.00	2.00
APSB	4668	91.8	6.5	clear	no	neg	neg	neg	855	857	857	856.33	1.15
APSB	4657	93.6	5	cloudy	yes	neg	neg	neg	-	-	-	-	-
APSB	4670	97.2	6	cloudy	yes	neg	neg	neg	-	-	-	-	-
APSB	4659	106.2	7.5	clear	slight	neg	neg	neg	854	858	855	855.67	2.08
APSB	4646(2)	106.2	7.5	clear	no	neg	neg	neg	835	835	835	835.00	0.00
APSB	4667	115.2	5.5	clear	no	neg	neg	neg	853	852	855	853.33	1.53
APSB	4646(f)	117	7.5	slightly cloudy	no	neg	neg	neg	855	854	856	855.00	1.00
APSB	4646(1)	198	7.5	clear	no	neg	neg	neg	848	849	845	847.33	2.08
APSB	4671	248.4	5.5	slightly cloudy	slight	2+ 1 g/L	neg	neg	845	844	845	844.67	0.58
APSB	4674		5	cloudy	yes	neg	neg	neg	-	-	-	-	-
APSB	4678		7.5	clear	no	neg	neg	neg	-	-	-	-	-
APSB	4684		7	clear	no	neg	neg	neg	-	-	-	-	-
APSB	4685		6	clear	no	neg	neg	neg	-	-	-	-	-
APSB	4686		6	clear	no	neg	neg	neg	-	-	-	-	-
APSB	4727		5.5	Cloudy	Yes	neg	neg	neg	-	-	-	-	-
APSB	4718	90	5.5	Clear	No	neg	neg	neg	867	872	869	869.33	2.52

APSB	4726	91.8	7	Slightly Cloudy	No	neg	neg	neg	842	849	846	845.67	3.51
APSB	4723	97.2	6.5	Clear	No	neg	neg	neg	867	869	869	868.33	1.15
APSB	4701	97.2	5.5	Cloudy	No	neg	neg	neg	-	-	-		
APSB	4703	99	6.5	Clear	No	neg	neg	neg	866	866	864	865.33	1.15
APSB	4702	104.4	5	Cloudy	No	neg	neg	neg	-	-	-		
APSB	4704	109.8	7.5	Clear	No	neg	neg	neg	869	869	867	868.33	1.15
APSB	4725	124.2	7.5	Slightly Cloudy	No	neg	neg	neg	853	851	851	851.67	1.15
APSB	4728	127.8	5	Slightly Cloudy	No	neg	neg	neg	850	846	851	849.00	2.65
APSB	4719	149.4	5.5	Clear	No	neg	neg	neg	854	851	847	850.67	3.51
APSB	4700	167.4	7	Clear	No	neg	neg	neg	846	842	844	844.00	2.00
APSB	4724	333	5.5	Clear	No	neg	neg	neg	836	837	838	837.00	1.00
APSB	4785	77.4	5.5	Clear	No	neg	neg	neg	869	873	864	868.67	4.51
APSB	4768	79.2	6.5	Slightly Cloudy	No	neg	neg	neg	-	-	-	-	-
APSB	4790	86.4	5.5	Slightly Cloudy	No	neg	neg	neg	868	866	861	865.00	3.61
APSB	4791	86.4	6.5	Slightly Cloudy	Slight	neg	neg	neg	-	-	-	-	-
APSB	4766	93.6	5.5	Clear	No	neg	neg	neg	861	859	851	857.00	5.29
APSB	4779	97.2	6.5	Clear	No	neg	neg	neg	862	863	859	861.33	2.08
APSB	4797	97.2	5	Clear	No	neg	neg	neg	845	849	849	847.67	2.31
APSB	4783	102.6	7.5	Clear	No	neg	neg	neg	867	867	862	865.33	2.89
APSB	4780	106.2	5.5	Clear	No	neg	neg	neg	871	870	869	870.00	1.00
APSB	4781	106.2	6.5	Clear	No	neg	neg	neg	859	853	853	855.00	3.46
APSB	4782	109.8	6.5	Slightly Cloudy	No	neg	neg	neg	852	853	853	852.67	0.58
APSB	4784	111.6	6	Clear	No	neg	neg	neg	872	865	875	870.67	5.13
APSB	4789	118.8	6	Slightly Cloudy	No	neg	neg	neg	849	849	848	848.67	0.58
APSB	4850	88.2	6.5	No	No	neg	neg	neg	879	869	872	873.33	5.13
APSB	4837	90	6	Cloudy	Yes	neg	neg	neg	-	-	-	-	-
APSB	4856	90	6.5	No	No	neg	neg	neg	865	862	863	863.33	1.53
APSB	4839	93.6	7.5	no	No	neg	neg	neg	847	850	848	848.33	1.53
APSB	4853	93.6	5.5	No	No	neg	neg	neg	839	841	843	841.00	2.00
APSB	4848	95.4	5.5	No	No	neg	neg	neg	863	861	-	862.00	1.41
APSB	4840(f)	97.2	7.5	Cloudy	Yes	neg	+- 0.5 mmol/L	neg	-	-	-	-	-
APSB	4843	97.2	7.5	No	No	neg	neg	neg	860	860	858	859.33	1.15
APSB	4845	99	5.5	No	Yes	neg	neg	neg	847	842	846	845.00	2.65
APSB	4846	104.4	7	No	No	neg	neg	neg	-	-	-	-	-
APSB	4841	106.2	7	No	No	neg	neg	neg	854	850	857	853.67	3.51
APSB	4854	115.2	5	Slight	Yes	neg	neg	neg	-	-	-	-	-
APSB	4844	135	6	No	No	2 + 1 g/L	+- 0.5 mmol/L	neg	834	838	833	835.00	2.65
APSB	4840(2)	165.6	7	No	No	neg	neg	neg	855	855	850	853.33	2.89
APSB	4840(1)	178.2	7	No	No	neg	neg	neg	839	846	849	844.67	5.13
APSB	4863	244.8	7.5	No	No	neg	neg	neg	845	845	842	844.00	1.73
APSB	4861	97.2	8.0	Clear	No	neg	neg	neg	865	866	865	865.33	0.58
APSB	4864	97.2	6.5	Clear	No	neg	neg	neg	868	864	865	865.67	2.08
APSB	4865	102.6	7.5	Clear	No	neg	neg	neg	867	864	866	865.67	1.53

APSB	4869	84.6	6.0	Slight	Yes	neg	neg	neg	-	-	-	-	-
APSB	4870	90.0	5.0	Clear	No	neg	neg	neg	860	860	867	862.33	4.04
APSB	4871	93.6	6.0	Slight	Yes	neg	neg	neg	-	-	-	-	-
APSB	4872	174.6	6.0	Clear	Slight	neg	neg	neg	847	843	843	844.33	2.31
APSB	4873	61.2	5.0	Clear	No	neg	neg	neg	874	872	871	872.33	1.53
APSB	4874	97.2	5.0	Clear	No	neg	neg	neg	864	868	861	864.33	3.51
APSB	4875	77.4	5.5	Clear	No	neg	neg	neg	869	866	869	868.00	1.73
APSB	4876	86.4	6.5	Cloudy	Slight	neg	neg	neg	-	-	-	-	-
APSB	4877	99.0	6.0	Cloudy	Yes	neg	neg	neg	-	-	-	-	-
APSB	4878	81.0	6.0	Slight	Slight	neg	neg	neg	-	-	-	-	-
APSB	4880	104.4	7.0	Clear	No	neg	neg	neg	869	862	863	864.67	3.79
APSB	4881	90.0	8.0	Clear	No	neg	neg	neg	867	863	866	865.33	2.08
APSB	4898	90.0	7.0	Clear	No	neg	neg	neg	865	868	864	865.67	2.08
APSB	6002	91.8	6.5	Clear	No	neg	neg	neg	870	868	868	868.67	1.15
PBP	b13	81		Cloudy	No				-	-	-	-	-
PBP	b17	84.6		Slightly Cloudy	No				-	-	-	-	-
PBP	b11	100.8		Clear	No				864	868	869	867.00	2.65
PBP	b5	113.4		Clear	No				866	864	865	865.00	1.00
PBP	b1	120.6		Clear	No				851	842	842	845.00	5.20
PBP	b9	122.4		Clear	No				850	854	850	851.33	2.31
PBP	b4	126		Clear	No				845	850	850	848.33	2.89
PBP	b2	133.2		Clear	No				849	848	848	848.33	0.58
PBP	b15	135		Slightly Cloudy	No				-	-	-	-	-
PBP	b3	138.6		Slightly Cloudy	No				-	-	-	-	-
PBP	b12	140.4		Slightly Cloudy	Yes				-	-	-	-	-
PBP	b18	156.6		Cloudy	No				-	-	-	-	-
PBP	b19	171		Clear	No				-	-	-	-	-
PBP	b7	176.4		Clear	No				845	845	850	846.67	2.89
PBP	b10	205.2		Clear	No				840	838	838	838.67	1.15
PBP	b16	234		Clear	No				835	832	833	833.33	1.53
PBP	b14	279		Clear	No				830	837	832	833.00	3.61
PBP	b8	487.8		Clear	No				820	817	818	818.33	1.53
PBP	c17	81							868	868	865	867.00	1.73
PBP	c3	84.6							872	869	864	868.33	4.04
PBP	c9	84.6							864	861	865	863.33	2.08
PBP	c17	86.4							864	862	862	862.67	1.15
PBP	c4	86.4							863	862	863	862.67	0.58
PBP	c11	88.2		Slightly Cloudy	Yes				843	846	849	846.00	3.00
PBP	c13	102.6		Cloudy	Yes				-	-	-	-	-
PBP	c20	115.2		Slightly Cloudy	No				838	838	830	835.33	4.62
PBP	c10	117							858	863	861	860.67	2.52
PBP	c12	118.8							858	862	860	860.00	2.00
PBP	c18	135							854	850	847	850.33	3.51
PBP	c5	142.2							840	842	848	843.33	4.16

PBP	c21	142.2							844	839	843	842.00	2.65
PBP	c7	156.6							845	841	841	842.33	2.31
PBP	c16	180							850	850	852	850.67	1.15
PBP	c19	180							838	838	836	837.33	1.15
PBP	c15	210.6		Cloudy	No				-	-	-	-	-
PBP	c14	286.2							835	830	830	831.67	2.89
PBP	c8	349.2							826	828	820	824.67	4.16

Fasting glucose levels that are considered positive for diabetes.

Samples unable to be used with smartphone-based laser refractometer.

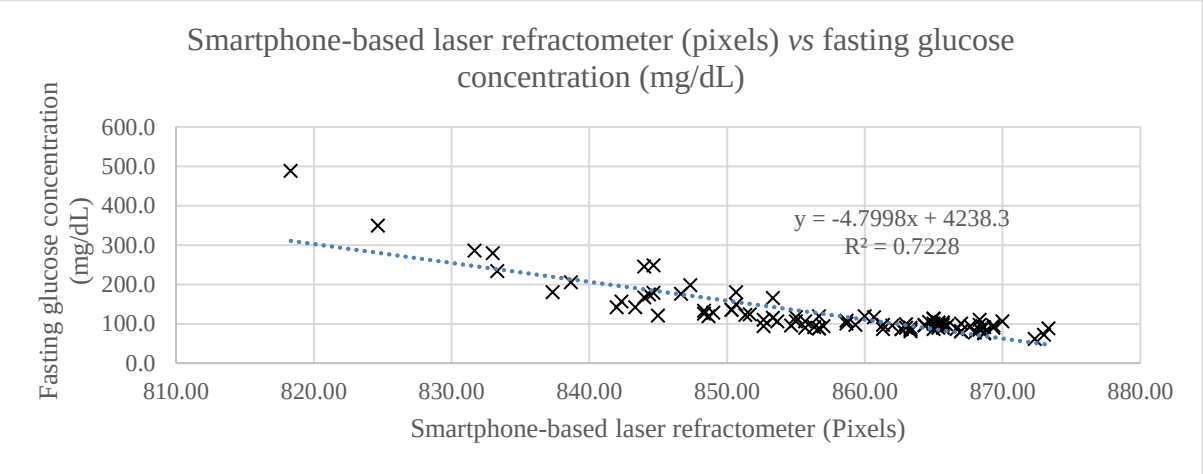

Figure B: Smartphone-based laser refractometer (pixels) *vs* fasting glucose concentration (mg/dL)